Nanoscale

REVIEW

View Article Online
View Journal | View Issue

Cite this: *Nanoscale*, 2025, **17**, 10411

Diverse applications of DNA origami as a cross-disciplinary tool

Lingyun Xiao, Xiaoxue Hu, Zhaoyu Zhou, Xiaolin Xie, Shujing Huang, Min Ji, Aobo Xu* and Ye Tian *

Received 29th October 2024,
Accepted 14th March 2025

DOI: 10.1039/d4nr04490h

rsc.li/nanoscale

As knowledge from a single discipline is no longer sufficient to keep pace with the growing complexity of technological advancements, interdisciplinary collaboration has become a crucial driver of innovation. DNA nanotechnology exemplifies this integration, serving as a field where cross-disciplinary communication is particularly prominent. Since its introduction by Rothemund in 2006, DNA origami has proved to be a powerful tool for interdisciplinary research, offering exceptional structural stability, programmability, and addressability. This review provides an overview of the development of DNA origami technology, highlights its major advances, and explores its innovative applications across various disciplines in recent years, showcasing its vast potential and future prospects. We believe DNA origami is poised for even broader applications, driving progress across multiple fields.

1 Introduction

Since the advent of the 21st century, relying solely on single-discipline knowledge has become increasingly inadequate for addressing the complex demands of scientific and technological progress. The integration of diverse disciplines has gradually provided greater inspiration for cutting-edge research and has become a significant driving force behind innovation in science and technology. Interdisciplinary research not only fosters the cross-fusion of ideas, methods, and technologies across different fields but also gives rise to numerous emerging disciplines. DNA nanotechnology, introduced by Seeman in 1982,[1] has since evolved into a dynamic arena for interdisciplinary integration, encompassing biology, chemistry, materials science, and other fields.[2–7] DNA molecules serve as an ideal template for interdisciplinary research due to their stable structure, predictable interactions, ease of modification with various inorganic and organic materials, and straightforward synthesis. Consequently, multiple disciplines have converged within this field. After more than two decades of progress, DNA origami technology, proposed by Rothemund in 2006, injected new vitality into this domain.[8] This innovative approach utilized the single-stranded DNA (ssDNA) of the M13mp18 phage, composed of more than 7 kilobases, as a scaffold, which was precisely folded by hundreds of staple strands. Through this technique, DNA undergoes a transformation from a self-assembled one-dimensional (1D) double helix to multidimensional structures, unlocking potential functional applications. The coding nature of DNA is founded on the Watson–Crick base-pairing principle of complementarity, along with its characteristic double-helix structure featuring a hydrophobic interior and negatively charged exterior. Additionally, DNA's dynamic hybridization ability, virtually unrestricted oligonucleotide sequence synthesis, and chemical stability have established it as an exceptionally successful template for programmed molecular self-assembly.[9] Over the last two decades, the mechanisms underlying DNA origami assembly have been thoroughly investigated and clarified. Today, various complex DNA origami-based nanomaterials can be synthesized with high precision.[10–12] As a nanostructure based on a bottom-up self-assembly strategy, DNA exhibits stable properties, excellent addressability, and

College of Engineering and Applied Sciences, State Key Laboratory of Analytical Chemistry for Life Science, Nanjing Jinling Hospital, Affiliated Hospital of Medical School, Nanjing University, Nanjing 210023, China. E-mail: ytian@nju.edu.cn, 495896458@qq.com

Ye Tian

Ye Tian holds a B.S. degree from Nanjing University, a M.S. degree from Institute of Chemistry, Chinese Academy of Sciences, and a PhD. degree from Stony Brook University. He was a postdoc at Columbia University and Brookhaven National Lab, before becoming a Professor at Nanjing University in 2017. His research interests include DNA origami technology, self-assembly of nanoparticles, and applying DNA assemblies into biology.

remarkable programmability, making it an increasingly valuable tool for interdisciplinary research.

Here, we highlight recent advancements in DNA origami within the interdisciplinary realm of DNA nanotechnology. We begin by outlining the development of DNA origami techniques and subsequently provide a comprehensive summary of the latest breakthroughs in their applications across various fields, showcasing their versatility and transformative potential. In materials science, DNA origami has enabled the fabrication of functionalized nanomaterials, such as DNA–silica composites, metal nanowires, and nanostructure substrates, by integrating precise self-assembly with chemical and physical methods. These advances open new possibilities for developing multifunctional nanoscale devices. In biology, DNA origami has significantly enhanced the sensitivity of detecting a wide range of substances, including short oligonucleotides, microRNAs, lipids, enzymes, and ions. In drug delivery systems, these improvements facilitate targeted therapies and enable the creation of nanoreactors for studying biological processes. In optics, DNA origami supports the development of nanophotonic systems and enhances techniques such as surface-enhanced Raman scattering (SERS). In robotics, DNA origami has enabled the construction of nanoscale robots capable of performing precise tasks, including medical interventions. Additionally, DNA origami demonstrates potential in computing and information science, contributing to innovations such as DNA-integrated circuits and biocomputing. Finally, we address both the challenges and future prospects of interdisciplinary applications in this domain.

2 DNA origami

First proposed by Rothemund in 2006, the DNA origami technique is a bottom-up strategy for the precise construction of nanoscale structures.[8] The resulting nanostructures consist of hundreds of different staples and a long scaffold, offering excellent addressability and programmability. Over the past 20 years, scientists have continuously explored and innovated in various directions, including design principles, design tools, assembly mechanisms, and application areas, thereby driving the continuous advancement of DNA origami technology. The most direct outcome of this progress is the increasing complexity and refinement of DNA origami patterns, evolving from the initial symmetrical two-dimensional (2D) shapes like squares and smiling faces[8] to asymmetrical 2D patterns such as Chinese maps[13] and dolphins,[14] multilayer three-dimensional (3D) structures,[15] hollow 3D structures,[16] and wireframe structures incorporating multi-arm junctions.[17] Additionally, dynamic structures capable of undergoing configuration transformations in response to external stimuli have been developed.[18] The design and exploration of these origami structures have fostered the integration of DNA nanotechnology with other fields, expanding the applicability of DNA nanostructures across interdisciplinary domains. In this section, we outline the evolution of DNA origami structures and highlight new structures or systems that have recently been applied.

2.1 DNA origami structures

Although atomic force microscopy (AFM) and scanning tunneling microscopy have enabled the manipulation of individual atoms, their stringent temperature and vacuum conditions limit their practicality. To control the growth of small molecules at the nanoscale and use them as fundamental units for multilevel structures, DNA, which self-assembles under relatively mild conditions, emerged as an ideal raw material for the bottom-up synthesis of nanomaterials with ordered molecular arrangements. The original DNA origami technology was designed to create highly complex nanostructures. Rothemund utilized parallel double helices to fill predetermined patterns based on the precise specificity of base pairing, producing a series of 2D basic patterns (Fig. 1A).[8] Additionally, variations in DNA origami staples allow for precise addressing and fluorescent labeling of specific sites, enabling the display of various images or text at a given resolution on the rectangular 2D origami template (Fig. 1B).[8] Building on this strategy, Qian *et al.* introduced a more intricate geographic pattern by designing block structures to fill asymmetrical areas, exemplified by the detailed borders of the Chinese map and its islands (Fig. 1C).[13] Han and collaborators expanded DNA origami strategies using partially complementary double-stranded DNA (dsDNA) and cohesive interactions of parallel crossovers. Unlike the traditional "staple" model, this novel construction method eliminates the need for auxiliary strands, allowing compact shapes, such as hearts and diamonds, to be formed by simply folding ssDNA (Fig. 1D).[19]

Beyond parallel raster stacking, a novel origami strategy directly constructs polygons using helix bundles composed of multiple dsDNA. Zhang and co-workers first created a variety of complex 2D wireframe origami structures using double crosses (DX) and double helix bundles (2HB) (Fig. 1E).[17] To assemble 2D geometries with more vertices and arbitrary edge lengths and curvatures, Jun *et al.* introduced a wireframe origami program based on automatic PERDIX generation (Fig. 1F).[20] By simply drawing the edges of a desired structure, the program generates optimized graph-theoretic scaffold routing, enabling the rapid and robust creation of nanoscale templates for drug delivery, nanophotonics, and biomolecular sensing. In contrast to the initial single-chain folding approach, Wang *et al.* employed a 6HB based on a multilayer honeycomb design to enhance the stiffness and planarity of 2D origami structures.[21] By maximizing the number of crossovers at each neighboring edge, they effectively counteracted the unintended curvature typically observed in a liquid-phase environment.

The dense DNA helix design facilitates the construction of higher-dimensional structures, extending beyond conventional staple-based connections between adjacent parallel scaffolds in the plane (Fig. 2A). DNA helix bundles are arranged in specific stacking patterns to form various hollow structures with storage space.[22] These bundles are predominantly stacked in honeycomb and square configurations. Douglas *et al.* leveraged both of these as template interfaces to develop the open-source caDNAno software, which automates staple design and sequence filling within a framework of preset geometrical parameters,

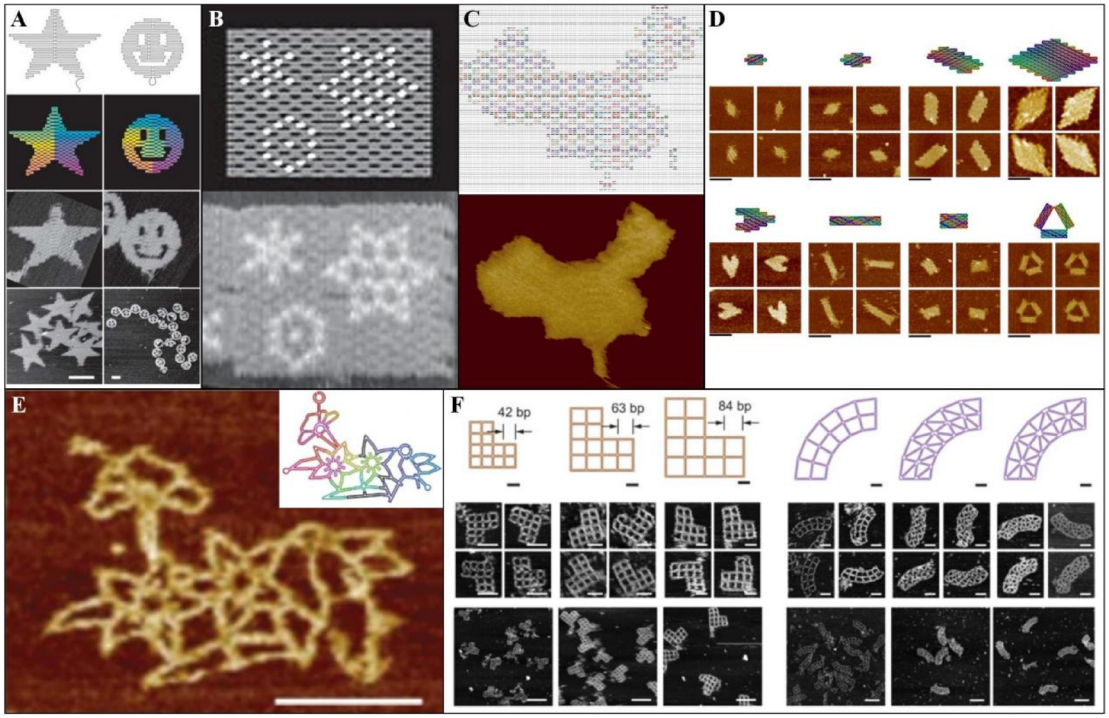

Fig. 1 DNA origami graphics obtained by different strategies. [A] Folding paths and AFM images of symmetric star and smiley face patterns. Scale bars: 100 nm. Reproduced from ref. 8 with permission from Springer Nature, copyright 2006. [B] Scaffold design and AFM image of the highlighted patterns on rectangular DNA origami structure. Reproduced from ref. 8 with permission from Springer Nature, copyright 2006. [C] Design of Chinese map origami graphic and AFM image. Shape is of ~150 nm length, ~120 nm width, and 2 nm height. Reproduced from ref. 13 with permission from Springer Nature, copyright 2006. [D] Various origami self-folding models with corresponding AFM images. Scale bars: 50 nm. Reproduced from ref. 19 with permission from AAAS, copyright 2017. [E] Scaffold folding path (upper right) and AFM images for flower-and-bird pattern. Scale bar: 100 nm. Reproduced from ref. 20 with permission from AAAS, copyright 2019. [F] AFM images of mesh patterns consisting of multi-arm junctions. Scale bars: 20 nm (model) and 50 (zoom-in) and 150 nm (zoom-out). Reproduced from ref. 21 with permission from AAAS, copyright 2022.

including double-helix diameter (2.0 nm), base pair length (0.34 nm), and helix period (10.5 base pairs).[23] Using caDNAno, researchers designed monoliths, square nuts (Fig. 2B), railed bridges, slotted crosses, stacked crosses, and numerous other structures. Dietz *et al.* extended the scope beyond highly symmetrical structures made from straight DNA helix bundles by introducing controlled bending and twisting through the strategic addition or removal of base pairs.[24] A 3 × 6 DNA helix bundle was designed to achieve a quasi-continuous bend ranging from 0° to 180°, progressing through seven incremental stages at 30° intervals (Fig. 2C). In contrast, Han and his collaborators pursued a different approach, producing in-plane curvature by constructing concentric circles of DNA while adjusting crossover positions to control out-of-plane curvature, ultimately achieving high-curvature nanostructures with low symmetry.[25] Using this strategy, representative nanospheres, ellipsoids, and nanoflasks were designed (Fig. 2D). Similar to wireframe structures, DNA origami has inspired new approaches for 3D construction. Benson *et al.* applied graph theory-based wiring algorithms and relaxation simulations for automated wiring, enabling the creation of complex structures that would have been challenging to achieve through traditional parallel alignment of DNA bundles.[16] Non-closed structures such as notched rings, spirals, and asymmetrical complex geometries—including rabbits—were designed in Autodesk Maya, and these hollow structures were visualized using cryo-electron microscopy (Fig. 2E). The development of new design software and construction strategies has injected fresh momentum into DNA origami, facilitating the creation of a diverse array of highly intricate multilayered structures while providing a solid theoretical foundation and expanded design space for future applications.

2.2 DNA origami assemblies

As the diversity of DNA origami structures has expanded significantly, researchers have set their sights on the next challenge in DNA nanotechnology: fabricating larger DNA structures. The maximum size of DNA origami is constrained by the 7249-nucleotide length of the M13mp18 phage, limiting 2D structures to 78 × 78 nm^2 and 3D structures to 24.7 × 24.7 × 24.7 nm^3.[26] To further increase the size of DNA origami structures, new scaffolds and techniques have been introduced, including phiX174,[27] λ-phage,[28] PCR amplification scaffolds,[29] and the conversion of dsDNA to ssDNA by pyromorphism.[26] These advancements have expanded the size of 2D origami monoliths to an area of 25 704 nm^2, with a side length of up to 300 nm.[30,31]

Adaptations based on DNA scaffolds have led to a broader design space but also increased costs and by-products. Nonetheless, synthesizing large structures with nanometer-

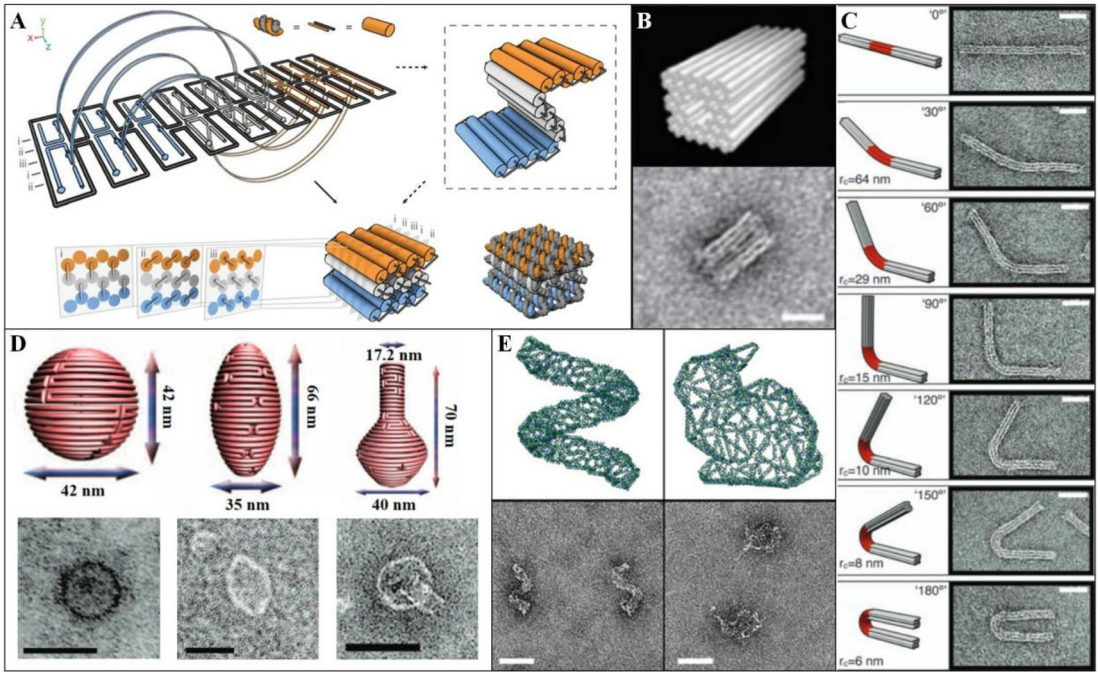

Fig. 2 DNA origami nanogeometry and 3D structures. [A] Schematic diagram of the construction strategy of 3D DNA origami. Reproduced from ref. 22 with permission from Springer Nature, copyright 2009. [B] Diagram and transmission electron microscope (TEM) image of square nut origami model. Scale bar: 20 nm. Reproduced from ref. 23 with permission from Oxford University Press, copyright 2009. [C] Schematic diagram and TEM image of the 3 × 6 helix bundle with different bending angles. Scale bars: 20 nm. Reproduced from ref. 24 with permission from AAAS, copyright 2009. [D] Model diagrams and TEM images of the DNA origami structures with 3D curvature. Scale bars: 50 nm. Reproduced from ref. 25 with permission from AAAS, copyright 2011. [E] 3D hollow origami wiring schematic and TEM image. Scale bars: 50 nm. Reproduced from ref. 16 with permission from Springer Nature, copyright 2015.

scale precision remains a challenge. The assembly of origami monomers with attached connectors into layered, advanced structures represents an innovative strategy for constructing micrometer-scale lattices. This approach leverages the combinatorial arrangement of monomers in one-, two-, or multiple-unit combinations to achieve complex configurations. The construction principles of assembly connectors fall primarily into two categories: DNA hybridization[8,32] and blunt-end stacking.[33] Wang *et al.* designed their assembly based on the sides of 6HB wireframe origami, creating bundle vacancies and extended sticky ends to form a superstructure using triangular wireframe origami as the core element (Fig. 3A).[34] This parallel-crossing assembly enables the construction of a compact, rigid 2D planar superstructure with potential applications in nanoscale lithography. Another assembly strategy, DNA reverse parallel ligation, is commonly used to hybridize the sticky ends of protruding single strands. Wang and colleagues developed a hexagonal origami tile that can be assembled into large 2D planes or honeycomb tubes of varying diameters by adjusting the number of complementary and gap bases in the sticky-end regions (Fig. 3B).[35] Incorporating Au nanoparticles (AuNPs) into the honeycomb lattice enabled the ordered arrangement of Au superlattices, exhibiting optical metamaterial properties and plasmonic resonances. Similarly, Liu *et al.* applied longer sticky ends to the vertices of square DNA origami structures, indirectly controlling monomer loop formation and planar quality by modulating the number of T bases in the spacer region of the sticky ends (Fig. 3C).[36]

Designs incorporating long T sequences between dsDNA bundles and sticky ends provide a flexible approach for attaching 3D hollow frameworks, enabling versatile structural configurations. Tian *et al.* reported a series of frame structures composed of 6HB or 10HB, co-assembled with various nanoparticles (NPs) such as AuNPs, quantum dots (QDs), and proteins (Fig. 3D).[37] This approach offers a general strategy for creating arrays of nano-objects using a consistent assembly process. Building on this foundation, a total of 85 DNA origami frame/AuNP superlattices were synthesized through the co-crystallization of multiple octahedral frameworks.[38] The DNA origami nano-chamber (DNC), designed by Lin *et al.*, encoded specific connections along three orthogonal axes while preserving cavities for molecular associations (Fig. 3E).[39] Bayrak *et al.* employed a similar strategy to produce highly homogeneous gold nanowires, with diameters of 20–30 nm, through ionic growth by tightly connecting chambers loaded with 5 nm AuNPs in a 1D arrangement.[40] Berengut *et al.* designed chiral nanotubes with varying degrees of twist and diameters by modifying alternating dihedral angles to control intrinsic sheet curvature.[41] Wickham *et al.* coaxially assembled DNA origami barrels to create precisely addressable decamers, functioning as 3D pegboards that isolate reaction environments inside and outside the barrels.[42]

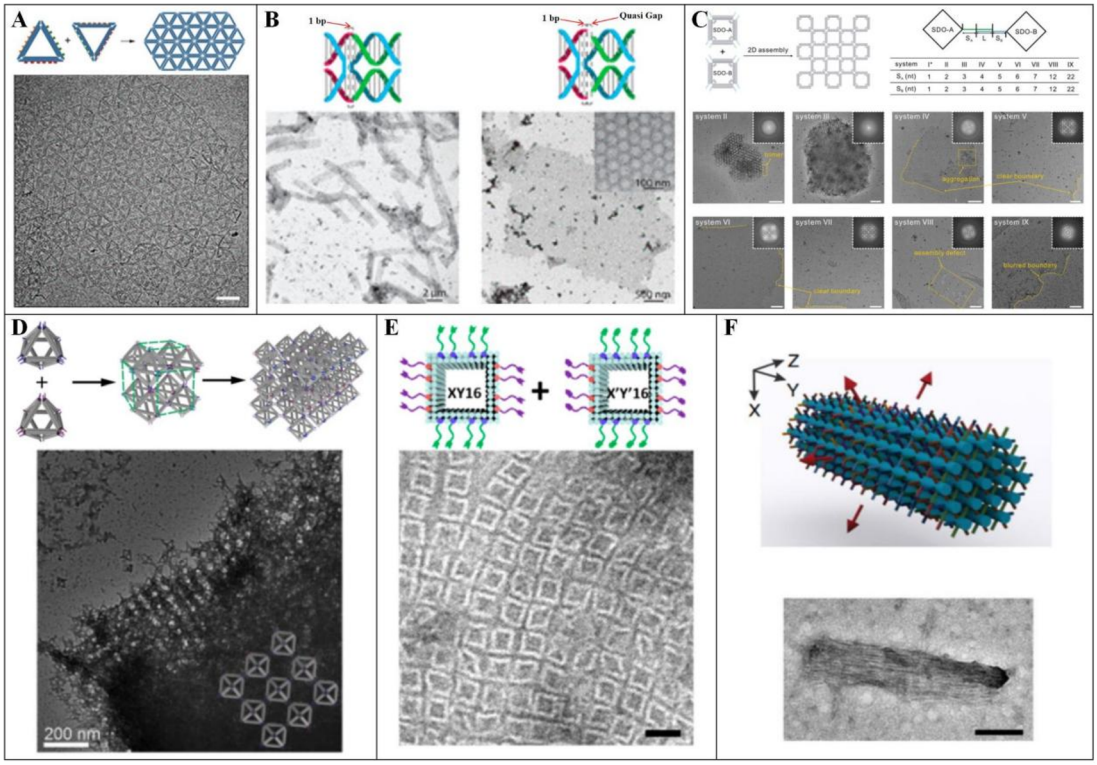

Fig. 3 Examples of DNA origami assemblies. [A] Schematic and TEM image of triangular array assembly. Scale bar: 100 nm. Reproduced from ref. 34 with permission from ACS, copyright 2022. [B] Sticky ends guide the assembly of DNA origami tiles into tubular or planar structures. Reproduced from ref. 35 with permission from ACS, copyright 2016. [C] T sequence regulates SDO ring formation and planar assembly. Scale bars: 500 nm. Reproduced from ref. 36 with permission from ACS, copyright 2024. [D] Schematic and TEM images of the 3D assembly of DNA origami octahedra. Reproduced from ref. 37 with permission from Springer Nature, copyright 2020. [E] Schematic and TEM images of DNC 2D assembly. Scale bar: 50 nm. Reproduced from ref. 39 with permission from ACS, copyright 2020. [F] Schematic and TEM images of 3D meta-DNA assemblies Scale bar: 100 nm. Reproduced from ref. 44 with permission from Springer Nature, copyright 2020.

To construct micron-sized DNA structures, researchers have explored various methods to amplify scaffolds[30] and optimize annealing conditions.[43] Yao *et al.* pioneered the use of submicron-sized six-helix bundle DNA origami nanostructures as building blocks. By mimicking DNA strand assembly behavior, they created micron-scale complex origami structures. Three self-assembly strategies—single-stranded tile assembly, single-stranded origami, and multi-arm junction tiles—were validated with meta-DNA, leading to the formation of larger 3D polyhedra and ribbons exceeding 5 μm in length (Fig. 3F).[44]

In addition to these methods, the degrees of freedom of adsorbed DNA origami monomers can be constrained to a 2D plane through interfaces such as solid–liquid,[45,46] liquid–air,[47] and lipid–liquid.[48] This surface-assisted strategy on mica sheets facilitates hierarchical DNA origami assembly *via* electrostatic interactions. By introducing an abundance of monovalent sodium ions, divalent magnesium ions at the mica–DNA interface are replaced, weakening the binding effect on DNA origami nanostructures. This reduction in binding enhances DNA origami mobility, allowing for more effective diffusion and alignment along the 2D surface.[45,46] Xin *et al.* utilized surface-assisted assembly on mica sheets to fabricate 2D lattices featuring densely packed rows with macroscopic-scale control. The ordered DNA origami lattice, extending up to 18.75 cm^2, was validated using fluorescence microscopy. Each DNA origami triangle was conjugated to a QD *via* streptavidin, and the uniformity of QD fluorescence served as an indicator of the lattice's structural order.[49] As a mask for molecular lithography, ordered monolayers of DNA origami structures can guide the adsorption of various proteins, including single-stranded annealing proteins like Redβ and Sak, the iron storage protein ferritin, and the blood protein bovine serum albumin (BSA).[50]

2.3 DNA origami purification

Purification is a critical step in obtaining high-quality DNA origami structures while preventing undesired aggregate formation. Agarose gel electrophoresis (AGE) is a widely used, high-resolution purification method that separates by-products based on their varying migration rates, allowing the recovery and enrichment of desired products by disrupting the gel.[51] However, AGE purification can result in significant sample loss. As an alternative, the polyethylene glycol (PEG) purification method has been proposed, offering a straightforward approach capable of achieving a purification level of over 99%.[52] Furthermore, to remove functional or fluorescent groups without introducing additional impurities, ultrafiltration filters provide adequate recovery and are well suited for purifying small quantities effectively.[53] For DNA–peptide polymers, purifi-

cation can be performed using reversed-phase high-performance liquid chromatography, where buffer exchanges yield pure samples; however, this method is cumbersome.[54] Ye *et al.* introduced a purification technique based on magnetic bead pull-down reactions to remove incompletely assembled structures, effectively separating fully assembled superstructures from excessive substructures.[55] By executing a multi-step pull-down reaction, desired superstructures can be meticulously isolated from assemblies or other inorganic NPs. W/W-droplet fractionation purification methods enable the rapid separation of macroscopic phases and enclosed molecules within seconds under centrifugation. This versatile technique can be applied to DNA origami structures of various sizes.[56] Additionally, other purification methods include size exclusion chromatography (SEC), gel filtration using rotary columns, and gradient ultracentrifugation. When selecting the appropriate purification method for a specific application, factors such as yield, purity, concentration, volume, residue, efficiency, and the method's impact on the sample should be carefully evaluated and compared.

3 Interdisciplinary applications

DNA origami provides an extraordinary ability to build micron-scale materials with sub-nanometer addressability. As a highly versatile platform characterized by significant programmability, it offers numerous chemically modified sites through pre-designed sequences, allowing precise control of nanoscale entities such as metal NPs, QDs, fluorescent dyes, and proteins. As a bridge, nanostructures fabricated using this bottom-up approach have the potential to facilitate advancements across various disciplines, leading to new discoveries and novel technological approaches in fields like materials science, biology, optics, robotics, and information science. This section discusses the diverse applications of DNA origami in these fields in recent years.

3.1 Interdisciplinary with material science

DNA is a synthetic biomaterial with self-assembling capabilities, and the presence of a phosphate backbone in the molecule imparts negative electrical properties. The elaborate high-dimensional structures created through DNA origami provide an excellent platform for fabricating advanced nanomaterials, exemplifying a quintessential case of interdisciplinary innovation. Silicon dioxide, metal nanoparticles, and metal oxide nanoparticles are integrated into complex structural or superlattice templates with the aid of DNA structures through various chemical methods, including chemical growth, atomic layer deposition (ALD), etching, and physical techniques like metal deposition and photolithography. These approaches collectively open up new possibilities for fabricating multifunctional devices at the nanoscale.

In 2009, Jin *et al.* introduced a novel approach for structural analysis under an electron microscope by constructing a DNA–silica complex (DSC).[57] By anchoring the trimethylene group of *N*-trimethoxysilylpropyl-*N*,*N*,*N*-trimethylammonium chloride (TMAPS) to the silicon atoms and the cationic ammonium group in the DSC, in the presence of the condenser quaternary ammonium group, the silane sites interacted with tetraethoxysilane (TEOS) to form a hard silica shell.[58] Auyeung *et al.* decoupled crystal parameters, such as symmetry and lattice spacing, of DNA-assembled superlattice crystals from the liquid-phase environment by silica encapsulation and obtained stable 10 nm gold nanoparticle lattices that did not deform, collapse, or dissociate under normal conditions.[59] The use of TMAPS and TEOS in DNA-encapsulated silica technology has been extensively studied, offering both theoretical insights and practical foundations for nanofabrication based on customized DNA origami templates.[60–62]

DNA origami, with its unique addressability as a structural material, has undergone extensive research and has proved to be an excellent customized template for fabricating DNA–silica composites. A surface-assisted two-step method was employed to silicify DNA origami by forming a silica shell of approximately 3 nm thickness on both small DNA origami structures and 2D lattices. The silica shell serves to protect the encapsulated DNA origami, ensuring that it maintains structural integrity even after being removed from a liquid-phase environment (Fig. 4A).[63] Nguyen *et al.* proposed an analogous sol–gel reaction to silicify larger 3D DNA origami crystals, resulting in silica shells with enhanced structural rigidity (Fig. 4B).[64] Jing *et al.* presented a DNA origami silicification (DOS) method for depositing silica onto the surface of DNA frameworks, allowing the formation of DNA–silica composites with more complex, programmable morphologies not limited to monolayers or multilayers of DNA origami with honeycomb lattice arrangements.[65] Shang *et al.* prepared silica patterns specifically on DNA origami templates designed with protruding strands at fixed positions. Differences in binding energies between prehydrolyzed products (PP)-dsDNA and PP-DNA origami were exploited, leading to preferential adsorption of PP onto the protruding dsDNA regions rather than the DNA origami surface.[66] Wassermann *et al.* reported a method that enables the specific addressing of silica cladding, allowing for the creation of dynamic silica nanostructures with precisely controllable shapes and sizes (Fig. 4C).[67] Wang *et al.* used a six-helix bundle DNA origami to explore how the presence of structural surface ssDNA and dsDNA affects the DNA origami during the silicification process. Crosslinking and aggregation of the origami structures were effectively prevented by ssDNA, allowing a thicker silica shell to form over a longer reaction time. Meanwhile, dsDNA facilitated the formation of silica on the surface of the DNA origami.[68] Additionally, Wang *et al.* achieved rapid silicification of DNA origami at a graphene interface, yielding a distortion-free 2D DNA origami–silica composite with twice the fidelity of bare DNA origami.[69]

Similarly, DNA origami acts as a structural template for the bottom-up synthesis of conducting metal nanowires. Continuous, complex metallic nanostructures are achieved through chemical growth between small metallic nanoparticles facilitated by reducing agents.[70] Common structures include metal nanowires used in electrical applications, such as gold,[71] silver,[72] palladium,[73] platinum,[74] copper,[75] nickel,[76] tellurium,[76] and cobalt nanowires,[77] which are typically

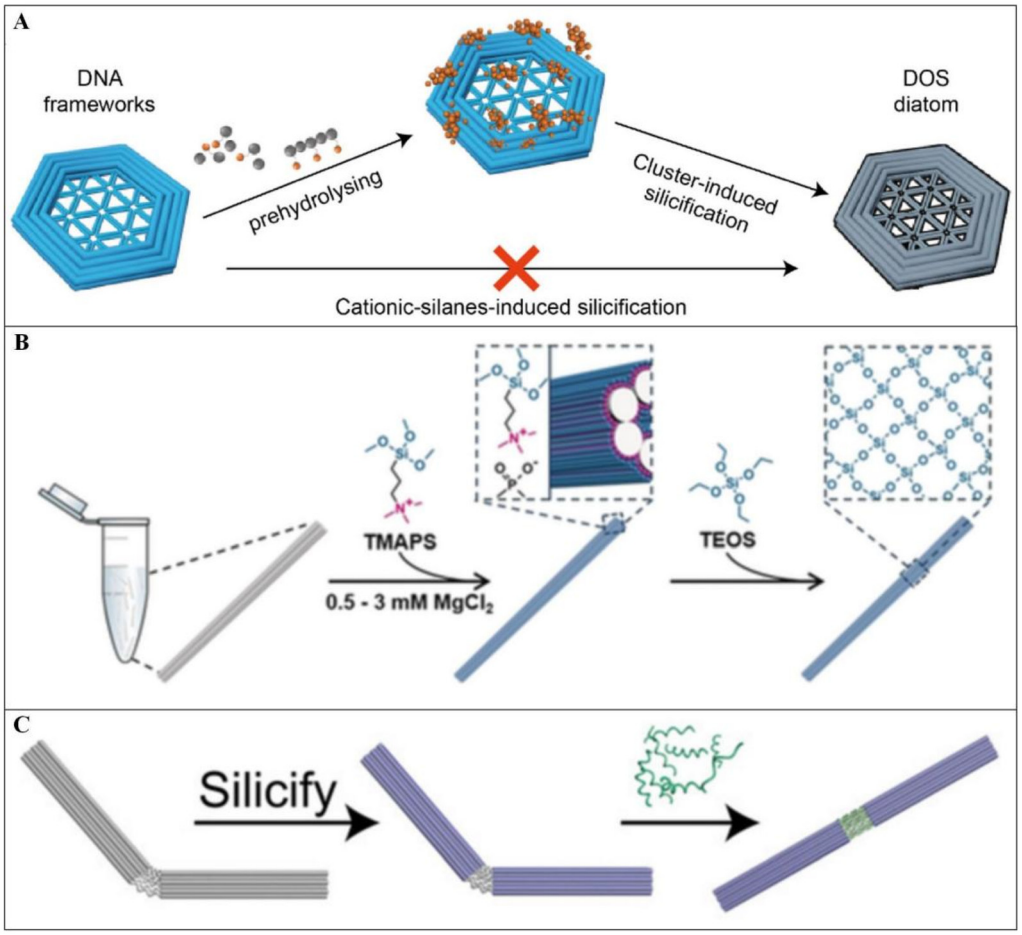

Fig. 4 Preparation of DNA origami silica composites. [A] DNA origami template-based guided growth of silica composites. Reproduced from ref. 63 with permission from Springer Nature, copyright 2018. [B] Schematic of DNA origami helix bundle package silicon. Reproduced from ref. 64 with permission from Wiley, copyright 2019. [C] Dynamic structure of 18HB with variable morphology before and after silicification. Reproduced from ref. 67 with permission from Wiley, copyright 2023.

formed through wet chemistry mediated by DNA templates. However, this approach has the limitation of providing only a restricted degree of control over the nanowires' shape. Yin *et al.* encapsulated gold nanoparticles in DNA origami molds containing cavities and introduced silver nitrate and ascorbic acid to limit the growth of silver monomers on the surface of the gold seeds, obtaining a series of gold-core–silver-shell structures with relatively controllable shapes (Fig. 5A).[78] This fabrication concept was later extended to casting triangular and disc-shaped structures and has also been applied to the synthesis of large-scale gold nanostructures.[78–80]

Jia *et al.* introduced a method that does not require exogenous metallic nanoparticles, instead inducing the formation of various metallic patterns based on the differing affinities of low-valent metal ions, such as Cu^{2+} and Ag^{+}, for protruding clustered DNA (pcDNA) and DNA origami substrates (Fig. 5B). This approach enabled the fabrication of nanoscale printed circuit boards with single and double layers.[81] Li and co-workers devised a patterning strategy relying on sulfhydryl-specific sites on DNA origami triangles, promoting the formation of proto-metal and metal–oxide nanoclusters (Fig. 5C).[82] In a similar vein, Zhang *et al.* employed DNA origami nanotubes, where diamine–silver complexes were locally enriched on specific single-stranded protruding clusters of DNA, resulting in chiral helix–silver patterns extending up to one micrometer in length (Fig. 5D).[83]

DNA nanostructures serve as highly adaptable templates for chemical vapor deposition (CVD) and ALD, enabling the fabrication of DNA origami–metal oxide complexes.[84] CVD, a widely used chemical technique, facilitates the production of monolayer or multilayer 2D materials by inducing gas-phase chemical reactions between precursors at elevated temperatures.[85] This method is particularly effective for creating large-scale, high-quality 2D materials, including graphene monolayers[86] and hexagonal boron nitride.[87] Surwade *et al.* achieved precise SiO_2 and TiO_2 deposition on DNA nanostructures with nanoscale resolution using a CVD method that regulated water adsorption at room temperature (Fig. 6A).[88] By controlling water adsorption at the nanoscale, they successfully manipulated the display of positive and negative tone patterns on DNA templates.

ALD, a technique derived from CVD,[89] relies on surface-specific chemical reactions for thin-film preparation.

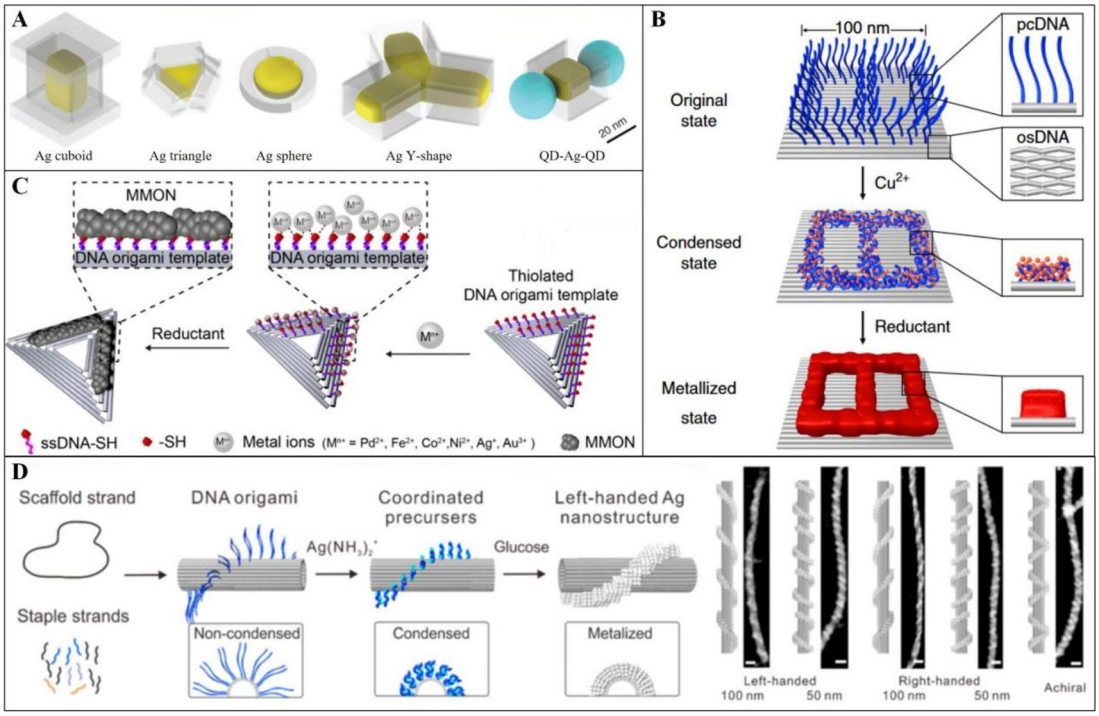

Fig. 5 Various metallization strategies based on DNA origami. [A] Casting NPs with form-fitting "box-lid" DNA origami molds. Reproduced from ref. 78 with permission from AAAS, copyright 2014. [B] High-resolution metal patterning on a single-origami breadboard by strong coordination of Cu^{2+} or Ag^{+} to pcDNA. Reproduced from ref. 81 with permission from Springer Nature, copyright 2019. [C] Synthesis of metal and metal oxide nanoclusters at specific sites on DNA origami triangles. Reproduced from ref. 82 with permission from ACS, copyright 2019. [D] Fabrication of chiral helical silver patterns and their assembly on DNA origami tubes. Reproduced from ref. 83 with permission from ACS, copyright 2021.

Compared with CVD, ALD offers advantages such as precise control over thin-film thickness, uniform coverage, and effective coating of complex structures at relatively low temperatures (<350 °C).[90–92] Posnjak *et al.* used ALD to modulate the thickness of a high-refractive-index titanium dioxide cladding layer on DNA origami diamond structures, achieving a complete photonic band gap (Fig. 6B).[93] Hui *et al.* employed ALD for regioselective Pt deposition mediated by DNA self-assembled structures, successfully fabricating various one- and two-component nanopatterns, including Pt, TiO_2/Pt, and Al_2O_3/Pt (Fig. 6C).[94]

Etching, a top-down micro- and nano-fabrication method, can be enhanced by incorporating DNA origami to produce metal nanostructures with improved continuity and structural integrity. DNA origami patterns can be deposited onto silica substrates, serving as masks similar to those used in photolithography. By integrating bottom-up and top-down fabrication approaches, this technique enables highly precise nanoscale fabrication. After etching with hydrogen fluoride vapor, the areas covered by DNA origami remain intact, resulting in patterns on the silica substrate that closely replicate the template's structure and shape.[95,96]

Since Seeman established the DNA molecular framework in 1982,[1] dsDNA and ssDNA have been extensively utilized as fundamental building units for self-assembled nanostructures, serving as fine material templates for region-selective metallization.[97] Dai *et al.* introduced a deposition strategy integrating silica–metal heterojunctions by leveraging the density and length of protruding dsDNA strands in DNA origami templates. This method enabled precise and addressable incorporation of silica–gold and silica–silver heterostructures.[98]

As electronic components continue to miniaturize, the line widths of integrated devices are shrinking, reaching as small as 5 nm through photolithography, which enables rapid, parallel, large-area fine processing. DNA origami holds significant potential as a surface lithography pattern mask due to the unique properties of its building blocks. DNA nanofabrication achieves a minimum size of 2 nm, making it an ideal candidate for precise nanoscale patterning. Shen's team introduced a modular epitaxy method for designing 3D DNA masks with programmable size, shape, and spacing. In this approach, a flat DNA brick crystal serves as the foundational surface for further assembly or modification, onto which 3D DNA modules grow in a seed-mediated manner. The DNA brick unit consists of a short 32-nucleotide DNA strand, allowing for a high resolution of 7 nm lateral critical size and 2 nm vertical critical size, which is preserved during DNA pattern transfer. The assembled 3D DNA mask is stabilized by Ni^{2+} ions, preventing feature collapse after air drying on silicon substrates. This Ni^{2+}-stabilized 3D DNA mask was then used to directly generate oversized Si patterns through a single run of reactive ion etching (RIE). The pitch and critical dimension (CD) of the

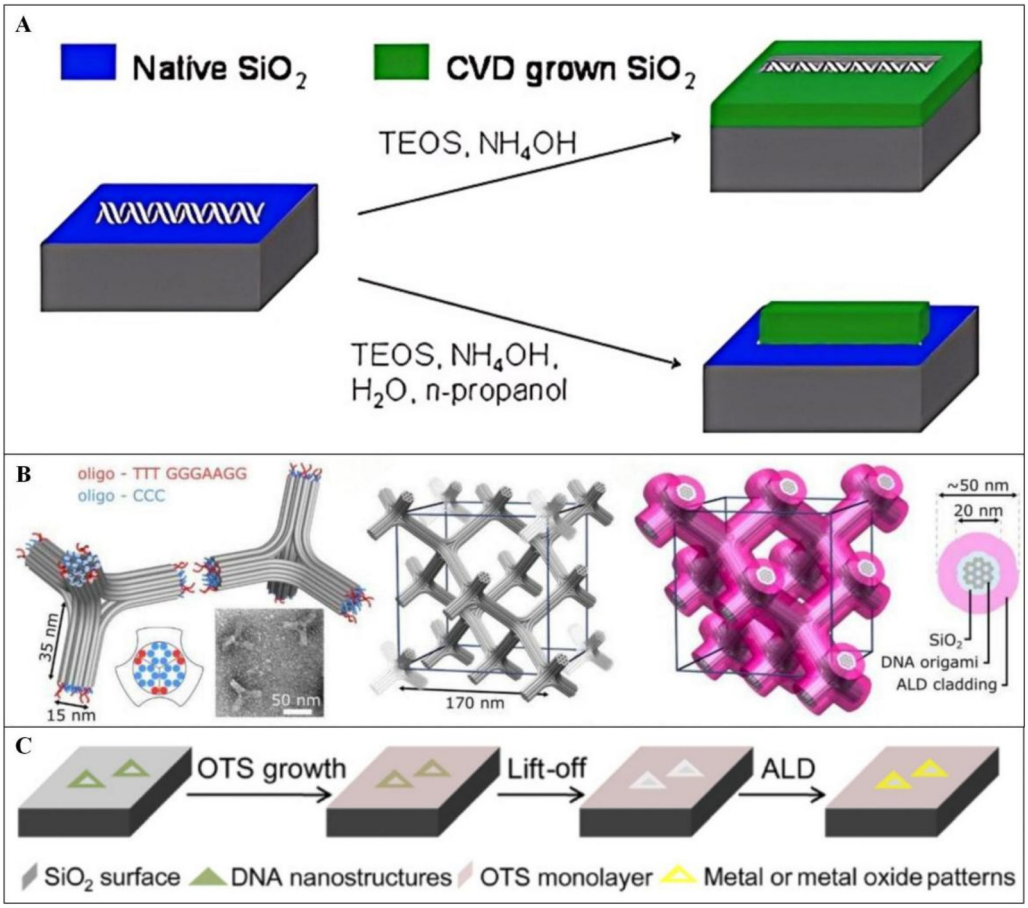

Fig. 6 Chemistry combined with DNA origami templates for nanofabrication processes. [A] Schematic representation of customised inorganic oxide nanostructures on DNA origami templates by CVD. Reproduced from ref. 88 with permission from ACS, copyright 2013. [B] Schematic representation of the assembly of DNA origami diamond cubic lattice and surface ALD growth of high refractive index cover layer. Reproduced from ref. 93 with permission from AAAS, copyright 2024. [C] Schematic representation of region-selective ALD preparation of Pt nanostructures based on DNA metal templates. Reproduced from ref. 94 with permission from ACS, copyright 2022.

Si patterns were reduced to 16.2 ± 0.6 nm and 7.2 ± 1.0 nm, respectively—a 50% reduction compared with current methods such as quadruple patterning or extreme ultraviolet (EUV) lithography.[99] This approach introduces a new technique for high-resolution silicon patterning on a wafer scale.

3.2 Interdisciplinary with biology

3.2.1 Sensing. The detection of biomarkers such as nucleic acids, lipids, ions, proteins, and other small molecules as quantifiable indicators is essential for disease prevention, early diagnosis, mid-term monitoring, and assessing treatment efficacy.[100] In nature, many biological processes rely on the precise positioning and orientation of interacting molecules. DNA nanotechnology offers a highly programmable and biocompatible framework for designing biosensing interfaces, allowing the precise spatial arrangement of molecules.[101] This unparalleled addressability enhances the sensitivity and specificity of detection systems in complex tissues and high-order biomolecules, creating exciting opportunities for developing advanced diagnostic tools and biosensors while improving the accuracy and efficiency of biological and medical tests.[102] To visualize detector metrics, four main strategies are commonly employed: (1) observing fluorescence resonance energy transfer (FRET) in DNA origami with precisely modified fluorescent moieties;[103] (2) directly monitoring morphology changes in DNA origami using AFM or TEM;[104–106] (3) detecting the plasmonic response of DNA origami–metal nanoparticle composites through alterations in optical properties;[107] and (4) detecting current changes induced by the translocation of nanopores constructed using DNA origami.[108] This section presents several detection strategies that employ functionalized DNA origami structures for various targets.

Due to its precise spatial addressability and numerous manipulable sites on the surface, DNA origami offers a novel solution for nucleic acid detection. Choi's group utilized DNA origami structures instead of traditional single-stranded DNA to attach dye molecules, combining this approach with planar microbead assays (Fig. 7A).[109] This method enables brighter and more sensitive quantitative measurement of target short

oligonucleotides at lower concentrations. The new reporter DNA origami expands the dynamic detection range and lowers the detection limit for oligonucleotides.

Dysregulated microRNA (miRNA) expression has been associated with cancer, and miRNA profiles have emerged as potential therapeutic targets.[110] Xing *et al.* developed an aptamer-tethered DNA origami amplifier that enables stable and highly sensitive detection of miRNAs in living cells (Fig. 7B).[111] Two substrate modules were assembled onto rectangular origami planes with edge-modified aptamers designed to target cancer cells. The presence of miRNA initiates sequential hybridization of the substrate modules, producing amplified and stable fluorescent signals *via* an intramolecular entropy-driven reaction.

Maingi *et al.* created a DNA origami ring-based nanoreactor that enables precise control of the connections between lipid-binding molecular receptors in three aspects: time, space, and stoichiometry.[112] This DNA origami-templated liposome (DOL) digital nanoreactor not only templates the synthesis of liposomes but also provides tethering sites for DNA-based receptors, potentially offering a customized instrument for studying and dissecting complex membrane protein interactions (Fig. 7C).

The dimensions of typical complementary metal oxide semiconductor (CMOS) devices closely match those of many biological systems. However, significant challenges remain in transmitting cellular biochemical signals to biosensors, primarily due to the insulating properties of cell membranes, which often result in considerable signal attenuation in extracellular measurements. To address this, Livernois *et al.* combined field-effect transistors (FETs) with DNA origami nanopores to create an ion detection device that can be seamlessly integrated into living cells.[113] The DNA nanopore forms an overlapping electrical double layer (EDL) that acts as a gate to the FET, achieving higher sensitivity than standard MOSFETs for single-ion detection.

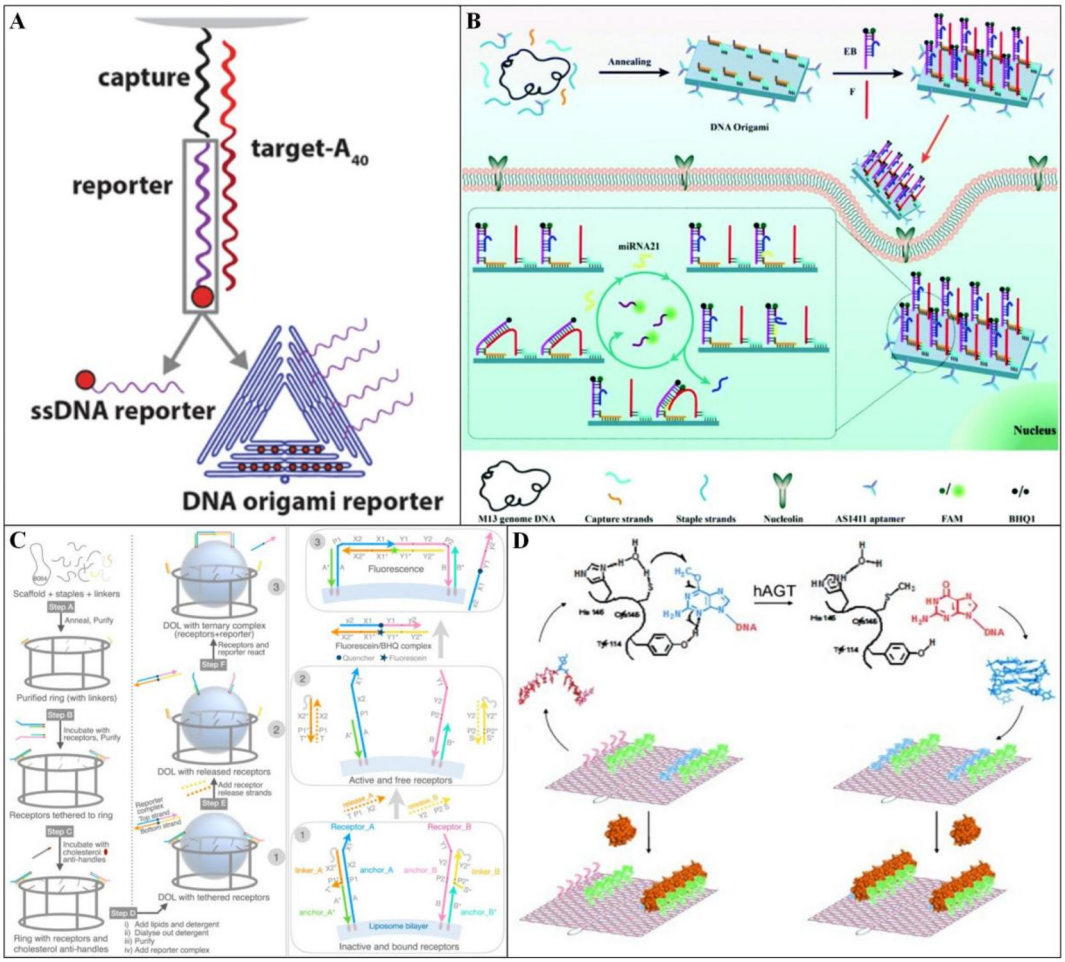

Fig. 7 DNA origami biosensors. [A] Microbeads are functionalized with streptavidin to which biotinylated capture DNAs are immobilized. Reproduced from ref. 109 with permission from Springer Nature, copyright 2019. [B] Model diagram of DNA origami amplifier. Reproduced from ref. 111 with permission from RSC, copyright 2022. [C] Schematic diagram of DOL assembly synthesis. Reproduced from ref. 112 with permission from Springer Nature, copyright 2023. [D] Schematic representation of the process by which hAGT repairs the methyl-TBA aptamer to symmetrically bind DNA origami quadruplexes to α-thrombin. Reproduced from ref. 114 with permission from Wiley, copyright 2013.

Tintoré *et al.* developed the first biosensor to visualize hAGT activity on an origami-based platform.[114] Their work applied single-molecule characterization of DNA origami for DNA repair assays by combining α-thrombin with TBA to determine the repair effect of hAGT on methylated TBA-origami (Fig. 7D). This platform lays the foundation for creating innovative biosensors that can detect the activity of various complexes and other proteins.

3.2.2 Drug delivery. In recent decades, drug delivery carrier materials have proliferated to expand the application of small-molecule drugs, addressing challenges such as low solubility, susceptibility to enzymatic and chemical degradation, and difficulty in crossing biological barriers.[115] DNA origami structures, with their inherent biocompatibility, ease of synthesis, abundance of modification sites, and highly flexible templates, have demonstrated significant potential for developing innovative targeted therapeutics, cancer treatments, and diagnostics.[116] A variety of therapeutic agents and materials, including antibiotics,[117] antigens,[118] immunostimulatory nucleotides,[119] therapeutic genes,[120] enzymes,[121,122] and lipid complexes,[123] can be loaded onto DNA origami molds through various interactions such as base pairing and covalent binding, expanding their potential in targeted delivery and personalized medicine.

Effective vaccine delivery with targeted transport and on-demand release remains a major challenge in cancer treatment. This has led to the development of delivery platforms based on programmable molecular systems, offering promising pathways for improvement. Liu's team designed a tubular DNA nanostructure to enable the precise assembly of two types of molecular adjuvants and antigenic peptides within its lumen, forming a vaccine (Fig. 8A).[124] A pH-sensitive DNA "locking strand" on the exterior of the tube allows the vaccine to open inside the lysosomes of antigen-presenting cells, effectively exposing the adjuvant and antigen to trigger a potent immune response.

The anthracycline doxorubicin (DOX) is a widely used anticancer drug known for its ability to intercalate into the DNA double helix, thereby inhibiting DNA replication and RNA synthesis, ultimately preventing cancer cell division. Zhang *et al.* non-covalently loaded DOX onto triangular origami structures (Fig. 8B). This DOX/origami therapy demonstrated enhanced anticancer efficacy in mammary tumors of BALB/c mice without causing systemic toxicity.[125]

Additionally, rapid advancements in technology have led to significant progress in the design of dynamic DNA origami devices, including nanorobots and nanoboxes with openable lids.[126] Ijäs and colleagues reported a pH-regulated dynamic DNA origami nanocapsule for studying enzyme-catalyzed reactions.[127] This capsule was equipped with multiple reversible "pH locks" for controlled switching and featured a functional cavity for anchoring molecules, effectively shielding the loaded cargo (Fig. 8C). Similarly, Douglas *et al.* designed dynamic nanodevices that can be activated in response to specific proteins on the cell surface, enabling the release of signaling molecules and the delivery of payloads such as Au NPs, antibodies, and more.[128]

Beyond cancer treatment, DNA origami has been explored for other diseases, including autoimmune disorders and bacterial infections. Li *et al.* developed a pH-responsive, dynamically reversible DNA origami structure that transitions from a closed to an open state, revealing a hexagonal array of CD95 ligands with molecular spacing of approximately 10 nm—matching the spatial configuration of CD95 receptor clusters on immune cell surfaces.[129] This design selectively activates CD95 death-inducing signals in immune cells within inflamed synovial tissue while sparing healthy hepatocytes in the liver, which express lower levels of CD95 receptors, thereby reducing hepatotoxicity. Wu and collaborators reported a bactericidal approach using DNA origami technology, in which DNA enzymes (G4/hemin) are precisely arranged on DNA origami to generate reactive oxygen species (ROS) in a controlled manner.[117] When combined with the broad-spectrum antibiotic levofloxacin, this method achieves highly effective bacterial killing. Additionally, the DNA origami-based bactericide enables targeted antimicrobial therapy through DNA aptamers that selectively bind to bacterial peptidoglycan, accelerating infected wound healing and presenting a novel approach for treating infectious diseases in living organisms.

3.3 Interdisciplinary with optics

In nano-optics, the precise control of various NPs in 3D space and time is essential for fabricating nanoscale optical components and presents a significant challenge in the field.[130] Metal NP cluster structures can manipulate light at the nanoscale, and such supramolecules, with spatially coupled atoms, have applications as potential metamaterials in nanocircuits, plasmonic sensors, subwavelength waveguides, and more. Fang *et al.* anchored AuNPs of varying sizes to rhombic origami templates to create supramolecular tetramers (Fig. 9A).[131] They found that Fano-like resonances in symmetric tetramers, identified using the dye SYBR Green I, resulted in a significant increase in electric intensity for SERS. The enhancement factor was further quantified using ROX as a Raman dye. Bald and collaborators investigated the effect of nanoparticle composition on the SERS performance of DNA origami nano-antennas based on DNA origami nanoforks.[132,133] By combining various shapes of Au or Ag NPs with DNA origami nanoforks, they successfully fabricated five different equilibrated excitonic nanoparticle dimers and systematically characterized their SERS intensities and enhancement factors at the single-dimer level. The study found that anisotropic nanoparticles featuring sharp edges, such as nanoflowers, significantly improved SERS performance and were particularly suitable for single-molecule SERS detection.

Semiconductor QDs are ideal materials for displays, lasers, transistors, photodetectors, and fiber optic communications due to their ability to emit tunable pure-colored light in the visible and near-infrared spectra, depending on their size. However, device applications require quantum rods (QRs) to be aligned along their long axis with nanoscale precision to achieve outcoupling efficiencies of up to 40% in LEDs.[134] DNA origami structures, with their excellent spatial addressability

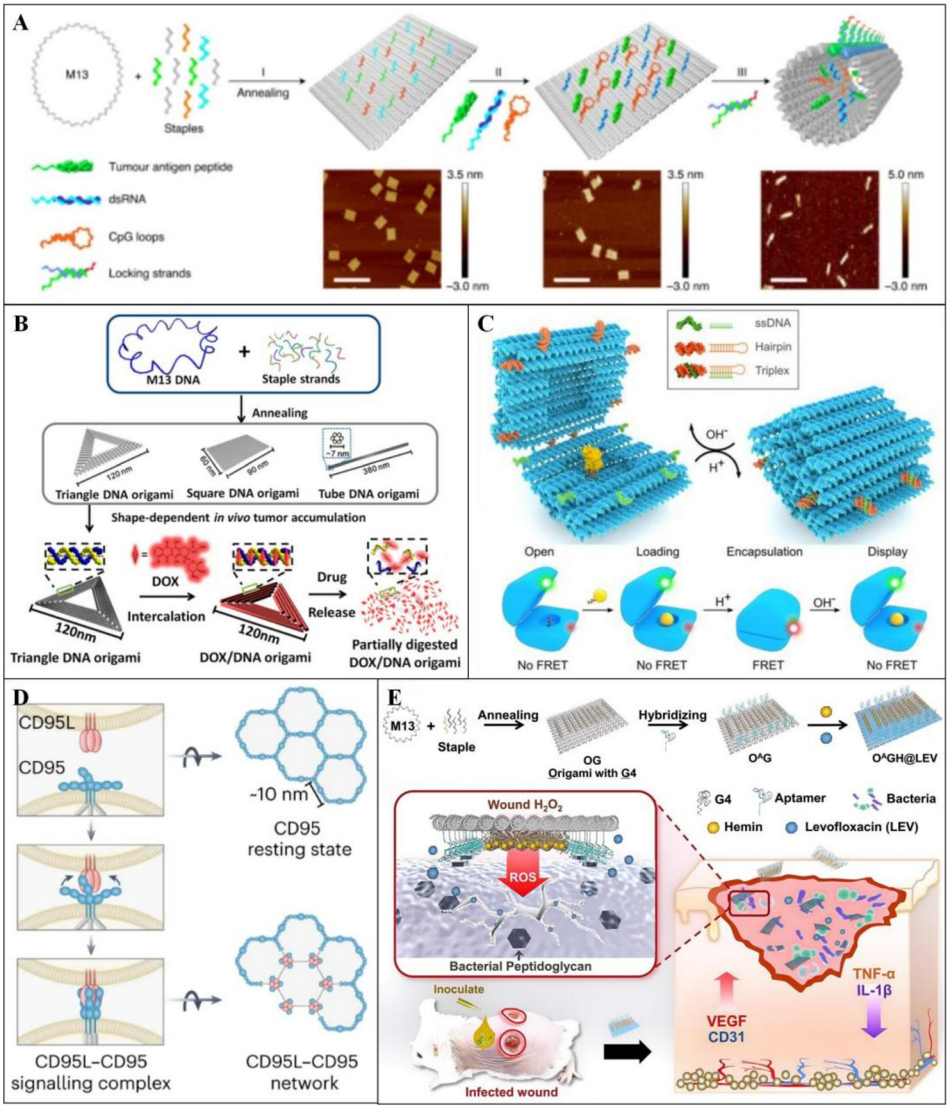

Fig. 8 DNA origami drug delivery devices. [A] Schematic illustration of the tumor antigen peptide/CpG loop/double-stranded RNA-encapsulated DNA origami robot. Scale bars: 200 nm. Reproduced from ref. 124 with permission from Springer Nature, copyright 2021. [B] Schematic design of the DNA carrier–drug complex. Reproduced from ref. 125 with permission from ACS, copyright 2014. [C] Schematic diagram of DNA origami nanocapsules. Reproduced from ref. 127 with permission from ACS, copyright 2019. [D] Hexagonal antiparallel dimer network modelling of CD95 receptor resting state. Reproduced from ref. 129 with permission from Springer Nature, copyright 2024. [E] Schematic of DNA origami nanoplatforms delivering DNAzyme and antibiotics against infection. Reproduced from ref. 117 with permission from Wiley, copyright 2023.

and programmability, offer a novel tool and method for the bottom-up assembly of nanophotonic systems. Chen *et al.* embedded monovalent QDs of varying sizes into wireframe origami structures, allowing accurate manipulation of the spatial arrangements between QDs and dyes (Fig. 9B).[135] By creating energy transfer circuits and colloidal molecules, they achieved control over the geometry and spatial addressing of QDs. This approach also integrates other materials, including dyes, to create nanophotonic devices, resulting in functional hybrid materials. Tinnefeld and co-workers pioneered fluorescence enhancement in DNA origami nanoantennas for signal amplification in single-molecule detection.[136] The main challenge in fluorescence-based diagnostics is distinguishing the signal from the background. While DNA origami nanoantennas enhance the photon budget of organic fluorophores, they do not overcome intrinsic limitations such as dark-state formation and photoinduced isomerization.[137] To address this, Yaadav *et al.* introduced QDs as an alternative, successfully capturing them in a hotspot formed by two 100 nm silver nanoparticles.[138] This setup resulted in broadband enhancement of QD fluorescence. Notably, QDs of different sizes exhibited significant fluorescence enhancement in the hotspots, with the smallest QDs showing more than a 100-fold fluorescence enhancement and a shortened fluorescence lifetime. This breakthrough offers a new approach for developing advanced equipartition excitation devices and customized bioassays.

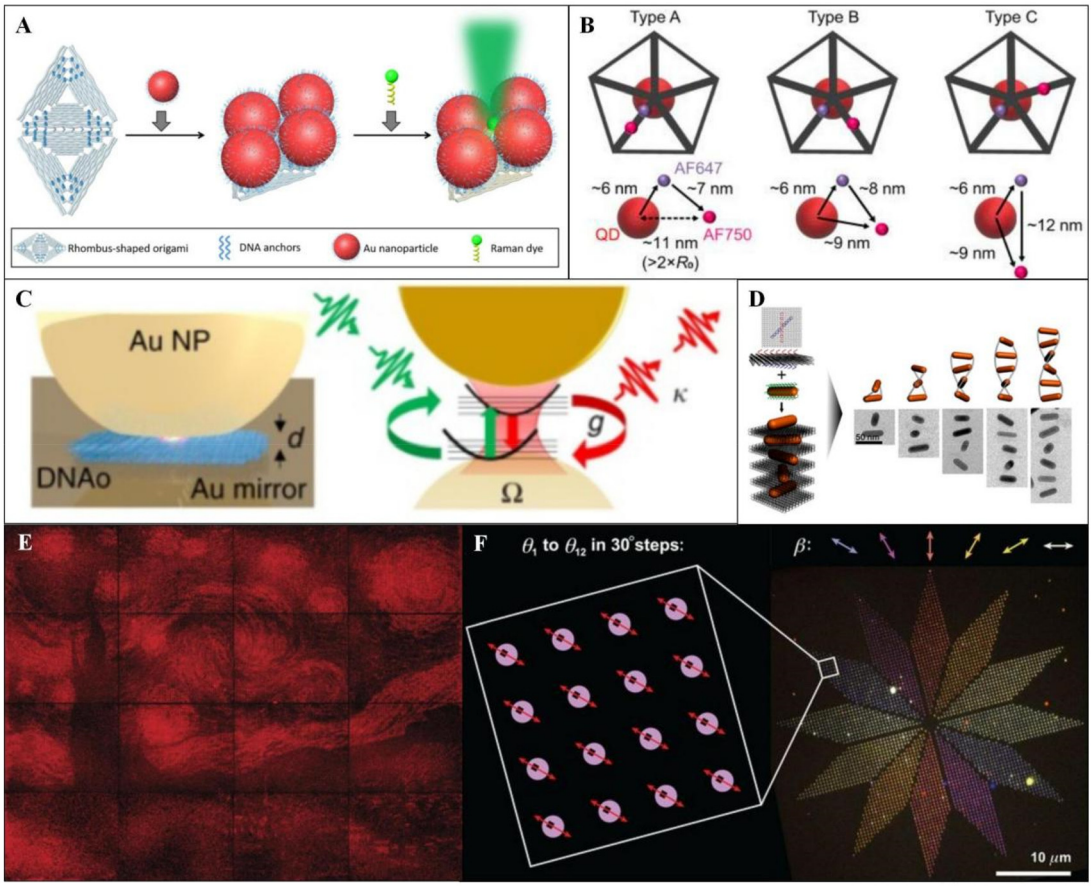

Fig. 9 The application of DNA origami and nanoparticle conjugates in the field of optics. [A] The process of immobilization of Au NPs and dyes by DNA hybridization on a rhombus-shaped origami. Reproduced from ref. 131 with permission from AAAS, copyright 2019. [B] Multistep transformation paths for fluorescent resonance energy transfer networks. Reproduced from ref. 135 with permission from Springer Nature, copyright 2022. [C] Schematic illustration of precision-located single molecule inside plasmonic cavity, with DNA origami as spacer. Reproduced from ref. 139 with permission from Springer Nature, copyright 2019. [D] Schematic of DNA-origami-assembled plasmonic helical superstructure composed of anisotropic AuNRs. Reproduced from ref. 140 with permission from ACS, copyright 2017. [E] Van Gogh's The Starry Night obtained by super-resolution mapping of origami placed in PCC. Reproduced from ref. 142 with permission from Springer Nature, copyright 2016. [F] 2D polarimeter composed of "small moon" shaped DNA origami labelled with fluorescent dyes. Reproduced from ref. 143 with permission from AAAS, copyright 2021.

The goal of quantum optics is to achieve strong coupling between cavities and single emitters. Among these, it is crucial to manufacture single-molecule nanocavities that operate at room temperature. Baumberg and co-workers used a single molecule of Atto647, aligned with DNA origami, to interact with a plasmonic nanocavity, exhibiting cooperative states (Fig. 9C).[139]

Metal nanostructures and their plasmon resonances are extensively utilized as optical transducers in sensing applications. When metal particles are closely positioned, they can couple to form a plasmon that supports collective electron oscillations. Circular dichroism (CD) spectroscopy, which is sensitive to minute conformational changes in the optical region *in situ*, can effectively reflect the optical response of plasmonic nanostructures comprising small metal particles. Zhou *et al.* proposed a plasmonic crossover structure capable of nanoscale conformational changes, forming a photostimulus-controlled system that switches between chiral locked and achiral relaxed states. To enhance the CD response, anisotropic Au nanorods (NRs) were used to fabricate chiral plasmonic crossover and helical superstructures (Fig. 9D).[140] Liedl and colleagues investigated both long-range and short-range chiral interactions in plasmonic nanoclusters constructed using DNA origami techniques, achieving CD signal amplification through the equi-isolated motif coupling of structural elements.[141] The team designed and synthesized a composite DNA origami structure incorporating two gold nanorods, with a third gold nanorod positioned between them to enable chiral signal transmission over long distances (up to approximately 100 nm). They experimentally verified the optical chiral properties of the structure, supported by numerical simulations. This work demonstrates the structure's potential applications in chiral sensors for biomolecules and chiral spin-locking in optical circuits.

Gopinath and collaborators proposed a precise placement technique using DNA origami to couple molecular emitters

with photonic crystal cavities, enabling exact control and mapping of nanocavity emission.[142] The study demonstrated how DNA origami can serve as a modular adapter to position emitters with high precision at various locations within a photonic crystal cavity, thus controlling both the emission intensity and the cavity mode. Furthermore, this technology enables the independent programming of thousands of photonic crystal cavities through large-scale integration, showcasing its vast potential for the rapid prototyping of nanophotonic devices.

Gopinath and co-workers reported an asymmetric "small moon"-shaped DNA origami with offset holes, achieved by stretching 20T ssDNA.[143] By exploiting the matching relationship between the overall shape of the DNA origami and photolithographically patterned binding sites, thousands of origami molecules were precisely oriented on a SiO_2 substrate. This orientation was accomplished both in an absolute manner, where all degrees of freedom were precisely defined, and in an arbitrary manner, where the orientation of each molecule was independently specified with an accuracy of ±3.2° in orientation. By integrating 3456 small crescent-shaped origami molecules labeled with TOTO-3 dye, they constructed a miniature fluorescence polarizer capable of distinguishing six different polarization directions. Furthermore, coupling these crescent-shaped origami molecules to a photonic crystal cavity (PCC) optimized the emission intensity by controlling the orientation of the origami, resulting in a 4.5-fold enhancement of the emission intensity.

3.4 Interdisciplinary with robotics

DNA origami structures rely primarily on reversible noncovalent interactions, specifically Watson–Crick base pairing and base stacking.[144] This reversibility has been exploited to design nanoscale robots, enabling precise mechanical manipulation through chain substitution reactions,[145] light irradiation,[146] thermal actuation,[147] pH-driven processes,[148] and other techniques.

To replace costly top-down nanomanipulation techniques, Benson *et al.* integrated three independently operated DNA origami linear actuators to construct a 2D-printed nanorobot using a bottom-up mechanical design strategy.[145] This device consists of a 2D origami canvas, a frame (comprising two base beams and a sliding rail), and a functional sleeve that selectively modifies pixels on the canvas. The sleeve introduces a signaling nucleotide that triggers a strand displacement reaction, displacing ink strands onto the canvas with high precision (Fig. 10A). Wang *et al.* developed a nanoscale DNA force spectrometer (nDFS) capable of reversibly switching hinge states with tunable mechanical and dynamic properties using DNA origami.[149] This system enables precise control at the nanoscale by applying tensile forces and pressures to individual molecules (Fig. 10B). Similarly, Mills and colleagues designed a DNA origami-based molecular actuator, the "nanowinch", which facilitates the parallel manipulation of multiple mechanoreceptors.[150] By leveraging adjustable single- and double-stranded DNA bonds, the nanowinch applies finely tuned low-piconewton forces in both autonomous and remote activation modes (Fig. 10C). This innovative method offers an instrument-free approach for studying cellular mechanical processes and exploring mechanotransduction circuits in living cells.

Integrating DNA origami platforms with molecular motors enables the creation of robots with virtually unlimited shapes and extensive functionalization capabilities. These nanomechanical systems perform various functions, including assembly,[151] sorting,[152] environmental response,[153] and directional transport[154] at the microscopic scale. However, to achieve fully autonomous and sustainable directional manipulation beyond externally driven motions, DNA-based autonomous molecular motors are necessary. Addressing this challenge, Siti *et al.* introduced a DNA molecular motor that drives a DNA walker along an origami surface, executing hybrid translational-rotational movements with high directional fidelity and remarkable speed (Fig. 10D).[155] Additionally, Ketterer *et al.* used multilayer DNA origami self-assembly to design a rotational mechanism that mimics biological rotating motors, undergoing conformational transitions without requiring an external energy source.[156] This mechanism enables random walks on docking points (Fig. 10E).

Zhou *et al.* created a DNA origami cube corner with DNA sticky-end edges, functioning as a robot controllable *via* ultraviolet light and temperature.[157] By modifying each face with AuNRs, the robot exhibited chiral and optical activity. Furthermore, it could self-assemble into complete cubes through a two-by-two assembly process and replicate itself within two cycles, enabling exponential growth in yield.

Wang and collaborators developed a DNA origami robotic switch that responds to the tumor microenvironment.[148] This switch autonomously displays cytotoxic ligand patterns that induce apoptosis in cancer cells within the acidic tumor environment while remaining inactive under normal physiological conditions. It demonstrated effective apoptosis induction in breast cancer cells *in vitro* and significantly inhibited tumor growth in a mouse model, presenting a promising strategy for precise tumor-targeted therapy.

Kopperger *et al.* reported an electrically driven nanoscale robotic arm, constructed *via* DNA self-assembly, that can reposition itself on a platform with millisecond precision.[158] This system enables rapid, electric field-driven transport of molecules or nanoparticles within milliseconds. Compared with conventional DNA hybridization reaction-driven systems, the electric field drive significantly enhances speed and efficiency, offering promising applications in molecular synthesis, assembly, photonics, and plasmonic process control.

3.5 Interdisciplinary with computer and information

Over the past few decades, computing technologies have evolved from specialized systems to general-purpose architectures, encompassing silicon-based computers, carbon nanotube-based computers, and quantum computers. The key to achieving general-purpose computing lies in programmability

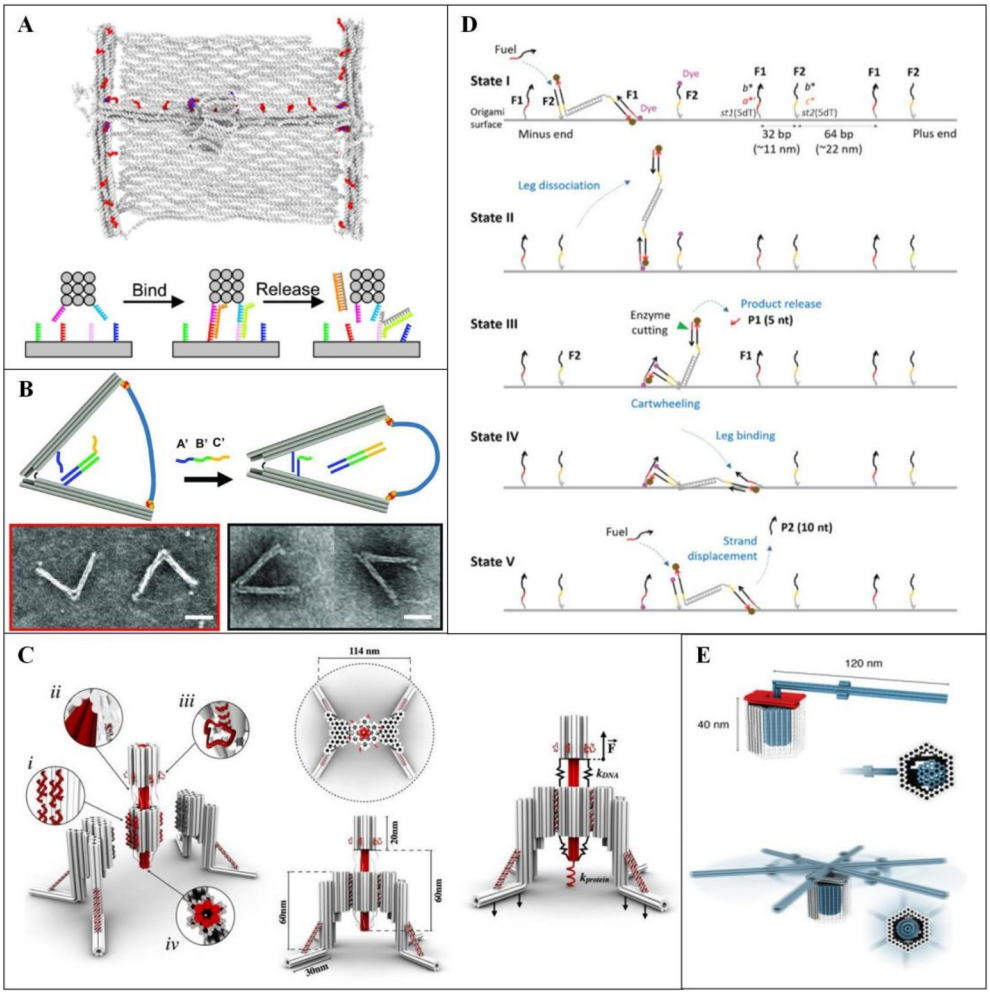

Fig. 10 Design of various DNA origami machines. [A] Schematic of the assembled 2D printed nanorobot and the controlled 2D printing process. Reproduced from ref. 145 with permission from AAAS, copyright 2022. [B] Schematic diagram of the working mechanism of an nDFS. Scale bars: 50 nm. Reproduced from ref. 149 with permission from Oxford University Press, copyright 2021. [C] A nano-winch assembled from honeycomb lattice DNA origami. Reproduced from ref. 150 with permission from Springer Nature, copyright 2022. [D] Schematic diagram of DNA bipedal motor operation. Reproduced from ref. 155 with permission from AAAS, copyright 2023. [E] A rotary DNA nanodevice composed of precisely interlocking 3D DNA components. Reproduced from ref. 156 with permission from AAAS, copyright 2016.

and scalability.[159] DNA-integrated circuits (DICs) are liquid-phase biocomputing systems that leverage biomolecular interactions to perform computations based on neuromorphic structures at the molecular level. These circuits have achieved breakthroughs in applications such as machine learning,[160] logic circuits,[161] decision-making machines[162] and neural networks.[163] Due to their programmability, immense parallel computing power, and compatibility with biological systems, DICs hold significant potential for broader applications and further generalization.

DNA-integrated circuits based on machine learning can accurately classify complex biological data, such as genomic, transcriptomic, and proteomic information, significantly improving the efficiency and effectiveness of medical diagnoses. This advancement has greatly enhanced the early detection of different cancer subtypes and stages.[164] Yang *et al.* accelerated cancer diagnosis by utilizing spatially constrained DNA origami frames (Fig. 11A). This approach prevents mutual interference between probes in different regions, reducing diagnosis time to as little as three hours—much faster than traditional diffusion-based systems.[165]

Fig. 11B illustrates dynamically interacting nanoscale robots constructed using DNA origami. These robots can switch states in response to specific protein cues, undergoing significant conformational changes to reveal internal payloads when gate chains are separated. By incorporating "positive regulators" (P) and "negative regulators" (N) as DNA keys, these robots can achieve mutual activation. Various configurations, designed by combining P and N robots with effector (E) robots in specific ratios, enable the simulation of a wide range of logic gate operations, including AND, OR, XOR, NAND, NOT, CNOT, and half-adders.[166] This innovative biocomputing platform is particularly suited for the controlled delivery of therapeutic molecules within living organisms, paving the way for

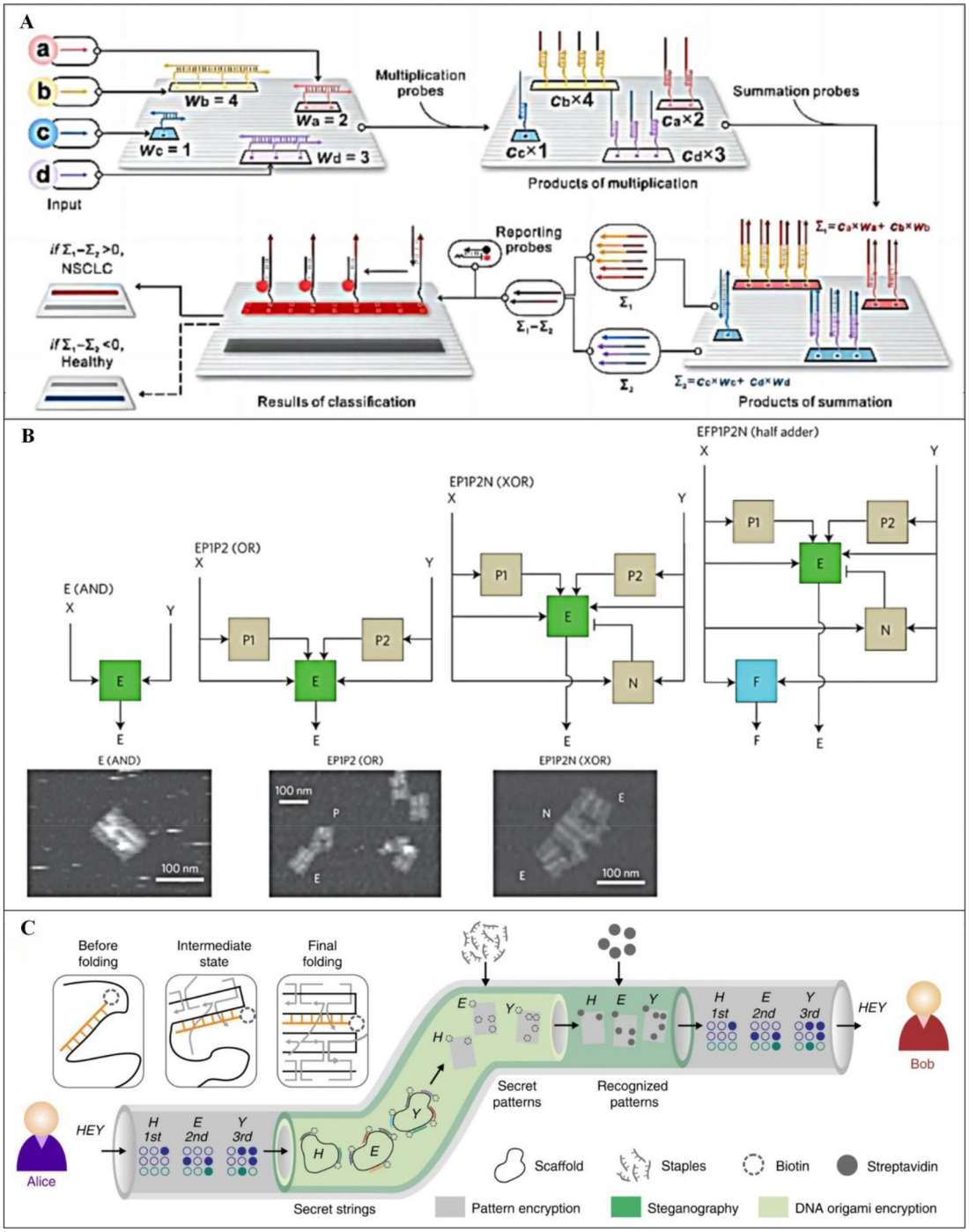

Fig. 11 [A] Schematic of the classification process of cancer diagnosis by utilizing miRNAs as input signals. Reproduced from ref. 165 with permission from Springer Nature, copyright 2024. [B] Robot emulates several logic gates in living animals. Reproduced from ref. 166 with permission from Springer Nature, copyright 2014. [C] Schematic diagram of the DOC security protocol. Reproduced from ref. 167 with permission from Springer Nature, copyright 2019.

computational regulation of human therapeutic processes and other biological functions.

With the growing importance of information security, the advent of quantum computers presents new challenges to cryptographic systems. DNA origami offers unique structural potential, expanding encryption protocols beyond traditional computational problems like factorization to include spatial structure folding. In 2019, Zhang *et al.* introduced a DNA origami cryptography (DOC) technique that utilizes self-assembled nanoscale Braille-like patterns for secure communication.[167] This method generates over 700-bit encryption keys and enhances confidentiality through protein-bound stegano-

graphy while ensuring message integrity and differential access control. The system supports a diverse range of data formats, including text, music notation, and images, demonstrating its versatility for secure communication across multiple mediums (Fig. 11C). In 2020, Fan *et al.* proposed an information encoding strategy based on reconfigurable DNA origami domino arrays.[168] This method enables conformational shifts within the arrays upon the introduction of a specific key, achieved through dynamic DNA units that rearrange intrinsic patterns for steganographic encryption while preserving overall array structure. Additionally, the strategy integrates encryption algorithms such as ASCII encoding to enhance security. Furthermore, a cryptographic anti-counterfeiting method, utilizing conformational transition-mediated chain substitution reactions, was introduced to ensure the complexity and unforgeability of encoded information. In 2024, Jiang *et al.* developed a subtraction-based encryption technique for DNA origami, where structural defects within the DNA origami framework are intentionally designed to store encrypted information.[169] Specific "hook" strands selectively remove target strands from a pool of intact staple strands, creating encrypted defective sites. These sites are then biotinylated with intact biotin molecules and incubated with a pool of biotinylated strands to form an encoded biotin pattern. Decryption is achieved through atomic force microscopy, which identifies the biotin markers. This approach demonstrates significant potential in biomolecular encryption and ensures a high level of message recovery accuracy.

4 Conclusions and future perspectives

Since the invention of DNA origami technology in 2006, researchers have explored this innovative approach to nanomaterial construction in diverse ways. Due to its high assembly precision, a wide variety of origami structures have been created for practical applications, establishing DNA origami as a key player across multiple fields. The phenomenon of interdisciplinary communication and integration occurs as DNA origami nanostructures serve as a bridge between numerous disciplines.[144] This includes not only the fields mentioned above but also emerging domains. Static and dynamic structures created with DNA origami have inspired advancements in photolithography and optical engineering, while DNA biocomputing systems have proved highly efficient for biochemical testing. Additionally, the fusion of DNA crystal frameworks with colloidal chemistry has led to the development of complex, porous structures.

Despite significant progress in creating DNA assemblies with programmable functionality, several challenges remain. Although DNA molecules are inherently biocompatible, the biotoxicity and potential antigenicity of DNA origami-based nano-assemblies must be carefully considered. The scaffold, derived from phage amplification, can retain lipopolysaccharide endotoxins that may trigger immunostimulatory effects in mammalian organisms. Furthermore, residual toxic chemicals such as agarose gel and ethidium bromide from the purification process must be addressed before DNA origami can be utilized as a drug delivery platform. When employed as a drug carrier, DNA origami faces challenges such as short blood residence time and limited ability to accumulate in target tissues due to elimination by cells and organs. In the realm of large-scale production and widespread application, DNA origami encounters challenges related to raw material costs, stringent environmental requirements, complex multi-step processes, and low structural yield.[170] Advances in biotechnology have reduced the cost of long-strand scaffolds to approximately $200 per gram and short-strand staples to under $300 per gram, making laboratory-scale preparation more feasible.[171,172] However, there remains a significant gap between this and the cost required for commercial production. Additionally, the stable existence of DNA origami structures depends on buffer salt solutions containing specific cations (*e.g.*, magnesium and sodium ions)[101] and maintaining a certain pH range.[173] When the solution deviates from these conditions, DNA origami structures may undergo unwanted hydrolysis, deformation, or denaturation.[174,175] Moreover, unstable ionic interactions and competition from secondary ions can disrupt the solution state of DNA origami monomers, leading to disordered aggregation and precipitation.[176–178] To address the technical challenges surrounding DNA structure strength and stability, various methods have been proposed, including silicification, metallization, protein cage encapsulation,[179] polyethylene glycolated oligo-lysine encapsulation,[180] co-assembly of protein polymers,[181] and UV spot welding for internal cross-linking.[182] These solutions could play a critical role in expanding the application of DNA origami nanostructures in the future.

In the coming decades, researchers are expected to push DNA origami technology into even more fields of study. For example, DNA origami could be constructed on a chip to integrate dynamic arrays of Au NPs, enabling rapid prototyping and the creation of nano-factories where individual components function similarly to living cells. DNA–NP conjugates can be assembled into 2D/3D patterns, liquid nanohydrogels, dynamic containers, bionic structures, and even avant-garde artwork, providing a new canvas for those with both scientific expertise and artistic creativity. The flexible joints, abundant binding sites, and negatively charged phosphate backbone of DNA nano-assemblies offer natural advantages for their use as nanoscale carriers. These carriers are capable of effectively delivering aptamers (*e.g.*, AS1411, MUC1, HApt),[183,184] antitumor drugs (*e.g.*, DOX, PTX, 5-FU),[185] immune factors (*e.g.*, CpG),[186] and fluorescent markers (*e.g.*, FAM), making them advanced nanotools for biosensing, bioimaging, and logic gate operations. As DNA origami technology merges with other advanced processing methods, nanostructures will increasingly influence macroscopic systems, enabling the creation of intricate constructs that were once deemed unfeasible. Furthermore, due to its inherent flexibility, DNA origami is expected to play a pivotal role in the development of innovative smart wearable devices. In summary, since its invention, DNA

origami technology has served as an ideal tool for fostering interdisciplinary connections. Through the integration of diverse concepts, theories, and methods, it has opened many previously unimaginable application pathways in DNA nanotechnology. We believe that, as interdisciplinary collaboration continues to deepen, DNA origami technology will lead to innovative applications across even more fields in the future.

Data availability

No primary research results, software or code have been included and no new data were generated or analysed as part of this review.

Conflicts of interest

The authors declare no conflict of interest.

Acknowledgements

This work is supported by the Fundamental Research Funds for the Central Universities (2024300319) and by the Program B for Outstanding PhD Candidates of Nanjing University (202402B15). The ToC was generated with permission from the American Chemical Society (copyright 2017, 2019, and 2021), The American Association for the Advancement of Science (copyright 2018), and John Wiley and Sons (copyright 2020).

References

1 N. C. Seeman, *J. Theor. Biol.*, 1982, **99**, 237–247.
2 A. Shaw, I. T. Hoffecker, I. Smyrlaki, J. Rosa, A. Grevys, D. Bratlie, I. Sandlie, T. E. Michaelsen, J. T. Andersen and B. Högberg, *Nat. Nanotechnol.*, 2019, **14**, 184–190.
3 S. Li, Q. Jiang, S. Liu, Y. Zhang, Y. Tian, C. Song, J. Wang, Y. Zou, G. J. Anderson, J.-Y. Han, Y. Chang, Y. Liu, C. Zhang, L. Chen, G. Zhou, G. Nie, H. Yan, B. Ding and Y. Zhao, *Nat. Biotechnol.*, 2018, **36**, 258–264.
4 F. Lu, H. Xin, W. Xia, M. Liu, Y. Zhang, W. Cai and O. Gang, *ACS Cent. Sci.*, 2018, **4**, 1742–1750.
5 Y. Chen, G. Ke, Y. Ma, Z. Zhu, M. Liu, Y. Liu, H. Yan and C. J. Yang, *J. Am. Chem. Soc.*, 2018, **140**, 8990–8996.
6 J. Wang, L. Yue, Z. Li, J. Zhang, H. Tian and I. Willner, *Nat. Commun.*, 2019, **10**, 4963.
7 M. Wang, L. Dai, J. Duan, Z. Ding, P. Wang, Z. Li, H. Xing and Y. Tian, *Angew. Chem., Int. Ed.*, 2020, **59**, 6389–6396.
8 P. W. K. Rothemund, *Nature*, 2006, **440**, 297–302.
9 M. Madsen and K. V. Gothelf, *Chem. Rev.*, 2019, **119**, 6384–6458.
10 Y. Wang, X. Yan, Z. Zhou, N. Ma and Y. Tian, *Angew. Chem., Int. Ed.*, 2022, **61**, e202208290.
11 X. Yan, Y. Wang, N. Ma, Y. Yu, L. Dai and Y. Tian, *J. Am. Chem. Soc.*, 2023, **145**, 3978–3986.
12 L. Dai, X. Hu, M. Ji, N. Ma, H. Xing, J.-J. Zhu, Q. Min and Y. Tian, *Proc. Natl. Acad. Sci. U. S. A.*, 2023, **120**, e2302142120.
13 L. Qian, Y. Wang, Z. Zhang, J. Zhao, D. Pan, Y. Zhang, Q. Liu, C. Fan, J. Hu and L. He, *Chin. Sci. Bull.*, 2006, **51**, 2973–2976.
14 E. S. Andersen, M. Dong, M. M. Nielsen, K. Jahn, A. Lind-Thomsen, W. Mamdouh, K. V. Gothelf, F. Besenbacher and J. Kjems, *ACS Nano*, 2008, **2**, 1213–1218.
15 T. Gerling, K. F. Wagenbauer, A. M. Neuner and H. Dietz, *Science*, 2015, **347**, 1446–1452.
16 E. Benson, A. Mohammed, J. Gardell, S. Masich, E. Czeizler, P. Orponen and B. Högberg, *Nature*, 2015, **523**, 441–444.
17 F. Zhang, S. Jiang, S. Wu, Y. Li, C. Mao, Y. Liu and H. Yan, *Nat. Nanotechnol.*, 2015, **10**, 779–784.
18 R. M. Zadegan, M. D. E. Jepsen, K. E. Thomsen, A. H. Okholm, D. H. Schaffert, E. S. Andersen, V. Birkedal and J. Kjems, *ACS Nano*, 2012, **6**, 10050–10053.
19 D. Han, X. Qi, C. Myhrvold, B. Wang, M. Dai, S. Jiang, M. Bates, Y. Liu, B. An, F. Zhang, H. Yan and P. Yin, *Science*, 2017, **358**, eaao2648.
20 H. Jun, F. Zhang, T. Shepherd, S. Ratanalert, X. Qi, H. Yan and M. Bathe, *Sci. Adv.*, 2019, **5**, eaav0655.
21 X. Wang, S. Li, H. Jun, T. John, K. Zhang, H. Fowler, J. P. K. Doye, W. Chiu and M. Bathe, *Sci. Adv.*, 2022, **8**, eabn0039.
22 S. M. Douglas, H. Dietz, T. Liedl, B. Högberg, F. Graf and W. M. Shih, *Nature*, 2009, **459**, 414–418.
23 S. M. Douglas, A. H. Marblestone, S. Teerapittayanon, A. Vazquez, G. M. Church and W. M. Shih, *Nucleic Acids Res.*, 2009, **37**, 5001–5006.
24 H. Dietz, S. M. Douglas and W. M. Shih, *Science*, 2009, **325**, 725–730.
25 D. Han, S. Pal, J. Nangreave, Z. Deng, Y. Liu and H. Yan, *Science*, 2011, **332**, 342–346.
26 Y. Yang, D. Han, J. Nangreave, Y. Liu and H. Yan, *ACS Nano*, 2012, **6**, 8209–8215.
27 Z. Zhao, Y. Liu and H. Yan, *Nano Lett.*, 2011, **11**, 2997–3002.
28 A. N. Marchi, I. Saaem, B. N. Vogen, S. Brown and T. H. LaBean, *Nano Lett.*, 2014, **14**, 5740–5747.
29 E. Pound, J. R. Ashton, H. A. Becerril and A. T. Woolley, *Nano Lett.*, 2009, **9**, 4302–4305.
30 H. Zhang, J. Chao, D. Pan, H. Liu, Q. Huang and C. Fan, *Chem. Commun.*, 2012, **48**, 6405–6407.
31 X. Chen, Q. Wang, J. Peng, Q. Long, H. Yu and Z. Li, *ACS Appl. Mater. Interfaces*, 2018, **10**, 24344–24348.
32 W. Liu, H. Zhong, R. Wang and N. C. Seeman, *Angew. Chem., Int. Ed.*, 2011, **50**, 264–267.
33 T. Zhang, C. Hartl, K. Frank, A. Heuer-Jungemann, S. Fischer, P. C. Nickels, B. Nickel and T. Liedl, *Adv. Mater.*, 2018, **30**, 1800273.
34 X. Wang, H. Jun and M. Bathe, *J. Am. Chem. Soc.*, 2022, **144**, 4403–4409.
35 P. Wang, S. Gaitanaros, S. Lee, M. Bathe, W. M. Shih and Y. Ke, *J. Am. Chem. Soc.*, 2016, **138**, 7733–7740.

36 Y. Liu, Z. Dai, X. Xie, B. Li, S. Jia, Q. Li, M. Li, C. Fan and X. Liu, *J. Am. Chem. Soc.*, 2024, **146**, 5461–5469.
37 Y. Tian, J. R. Lhermitte, L. Bai, T. Vo, H. L. Xin, H. Li, R. Li, M. Fukuto, K. G. Yager, J. S. Kahn, Y. Xiong, B. Minevich, S. K. Kumar and O. Gang, *Nat. Mater.*, 2020, **19**, 789–796.
38 M. Ji, Z. Zhou, W. Cao, N. Ma, W. Xu and Y. Tian, *Sci. Adv.*, 2022, **8**, eadc9755.
39 Z. Lin, H. Emamy, B. Minevich, Y. Xiong, S. Xiang, S. Kumar, Y. Ke and O. Gang, *J. Am. Chem. Soc.*, 2020, **142**, 17531–17542.
40 T. Bayrak, S. Helmi, J. Ye, D. Kauert, J. Kelling, T. Schönherr, R. Weichelt, A. Erbe and R. Seidel, *Nano Lett.*, 2018, **18**, 2116–2123.
41 J. F. Berengut, J. C. Berengut, J. P. K. Doye, D. Prešern, A. Kawamoto, J. Ruan, M. J. Wainwright and L. K. Lee, *Nucleic Acids Res.*, 2019, **47**, 11963–11975.
42 S. F. J. Wickham, A. Auer, J. Min, N. Ponnuswamy, J. B. Woehrstein, F. Schueder, M. T. Strauss, J. Schnitzbauer, B. Nathwani, Z. Zhao, S. D. Perrault, J. Hahn, S. Lee, M. M. Bastings, S. W. Helmig, A. L. Kodal, P. Yin, R. Jungmann and W. M. Shih, *Nat. Commun.*, 2020, **11**, 5768.
43 Y. Wang, L. Dai, Z. Ding, M. Ji, J. Liu, H. Xing, X. Liu, Y. Ke, C. Fan, P. Wang and Y. Tian, *Nat. Commun.*, 2021, **12**, 3011.
44 G. Yao, F. Zhang, F. Wang, T. Peng, H. Liu, E. Poppleton, P. Šulc, S. Jiang, L. Liu, C. Gong, X. Jing, X. Liu, L. Wang, Y. Liu, C. Fan and H. Yan, *Nat. Chem.*, 2020, **12**, 1067–1075.
45 A. Aghebat Rafat, T. Pirzer, M. B. Scheible, A. Kostina and F. C. Simmel, *Angew. Chem., Int. Ed.*, 2014, **53**, 7665–7668.
46 S. Woo and P. W. K. Rothemund, *Nat. Commun.*, 2014, **5**, 4889.
47 Y. Yonamine, K. Cervantes-Salguero, K. Minami, I. Kawamata, W. Nakanishi, J. P. Hill, S. Murata and K. Ariga, *Phys. Chem. Chem. Phys.*, 2016, **18**, 12576–12581.
48 Y. Suzuki, M. Endo and H. Sugiyama, *Nat. Commun.*, 2015, **6**, 8052.
49 Y. Xin, B. Shen, M. A. Kostiainen, G. Grundmeier, M. Castro, V. Linko and A. Keller, *Chem. – Eur. J.*, 2021, **27**, 8564–8571.
50 S. Ramakrishnan, S. Subramaniam, A. F. Stewart, G. Grundmeier and A. Keller, *ACS Appl. Mater. Interfaces*, 2016, **8**, 31239–31247.
51 G. Bellot, M. A. McClintock, C. Lin and W. M. Shih, *Nat. Methods*, 2011, **8**, 192–194.
52 E. Stahl, T. G. Martin, F. Praetorius and H. Dietz, *Angew. Chem., Int. Ed.*, 2014, **53**, 12735–12740.
53 A. Shaw, E. Benson and B. Högberg, *ACS Nano*, 2015, **9**, 4968–4975.
54 A. Buchberger, C. R. Simmons, N. E. Fahmi, R. Freeman and N. Stephanopoulos, *J. Am. Chem. Soc.*, 2020, **142**, 1406–1416.
55 J. Ye, J. Teske, U. Kemper and R. Seidel, *Small*, 2021, **17**, e2007218.
56 M. K. Masukawa, Y. Sato, F. Yu, K. Tsumoto, K. Yoshikawa and M. Takinoue, *ChemBioChem*, 2022, **23**, e202200240.
57 C. Jin, L. Han and S. Che, *Angew. Chem., Int. Ed.*, 2009, **48**, 9268–9272.
58 S. Che, A. E. Garcia-Bennett, T. Yokoi, K. Sakamoto, H. Kunieda, O. Terasaki and T. Tatsumi, *Nat. Mater.*, 2003, **2**, 801–805.
59 E. Auyeung, R. J. Macfarlane, C. H. J. Choi, J. I. Cutler and C. A. Mirkin, *Adv. Mater.*, 2012, **24**, 5181–5186.
60 B. Liu, L. Han and S. Che, *Angew. Chem., Int. Ed.*, 2012, **51**, 923–927.
61 B. Liu, Y. Yao and S. Che, *Angew. Chem., Int. Ed.*, 2013, **52**, 14186–14190.
62 Y. Cao, K. Kao, C. Mou, L. Han and S. Che, *Angew. Chem., Int. Ed.*, 2016, **55**, 2037–2041.
63 X. Liu, F. Zhang, X. Jing, M. Pan, P. Liu, W. Li, B. Zhu, J. Li, H. Chen, L. Wang, J. Lin, Y. Liu, D. Zhao, H. Yan and C. Fan, *Nature*, 2018, **559**, 593–598.
64 L. Nguyen, M. Döblinger, T. Liedl and A. Heuer-Jungemann, *Angew. Chem., Int. Ed.*, 2019, **58**, 912–916.
65 X. Jing, F. Zhang, M. Pan, X. Dai, J. Li, L. Wang, X. Liu, H. Yan and C. Fan, *Nat. Protoc.*, 2019, **14**, 2416–2436.
66 Y. Shang, N. Li, S. Liu, L. Wang, Z.-G. Wang, Z. Zhang and B. Ding, *Adv. Mater.*, 2020, **32**, 2000294.
67 L. M. Wassermann, M. Scheckenbach, A. V. Baptist, V. Glembockyte and A. Heuer-Jungemann, *Adv. Mater.*, 2023, **35**, 2212024.
68 S. Wang, P.-A. Lin, M. DeLuca, S. Zauscher, G. Arya and Y. Ke, *J. Am. Chem. Soc.*, 2024, **146**, 358–367.
69 H. Wang, Z. Li, X. Liu, S. Jia, Y. Gao and M. Li, *ACS Appl. Bio Mater.*, 2024, **7**, 2511–2518.
70 S. K. Vittala and D. Han, *ACS Appl. Bio Mater.*, 2020, **3**, 2702–2722.
71 B. R. Aryal, T. R. Westover, D. R. Ranasinghe, D. G. Calvopiña, B. Uprety, J. N. Harb, R. C. Davis and A. T. Woolley, *Langmuir*, 2018, **34**, 15069–15077.
72 S. K. Vittala, Y. Zhao and D. Han, *ChemPlusChem*, 2022, **87**, e202100478.
73 J. Richter, M. Mertig, W. Pompe, I. Mönch and H. K. Schackert, *Appl. Phys. Lett.*, 2001, **78**, 536–538.
74 R. Seidel, L. Colombi Ciacchi, M. Weigel, W. Pompe and M. Mertig, *J. Phys. Chem. B*, 2004, **108**, 10801–10811.
75 C. F. Monson and A. T. Woolley, *Nano Lett.*, 2003, **3**, 359–363.
76 J. Liu, B. Uprety, S. Gyawali, A. T. Woolley, N. V. Myung and J. N. Harb, *Langmuir*, 2013, **29**, 11176–11184.
77 Q. Gu and D. T. Haynie, *Mater. Lett.*, 2008, **62**, 3047–3050.
78 W. Sun, E. Boulais, Y. Hakobyan, W. L. Wang, A. Guan, M. Bathe and P. Yin, *Science*, 2014, **346**, 1258361.
79 T. Bayrak, S. Helmi, J. Ye, D. Kauert, J. Kelling, T. Schönherr, R. Weichelt, A. Erbe and R. Seidel, *Nano Lett.*, 2018, **18**, 2116–2123.
80 S. Helmi, C. Ziegler, D. J. Kauert and R. Seidel, *Nano Lett.*, 2014, **14**, 6693–6698.
81 S. Jia, J. Wang, M. Xie, J. Sun, H. Liu, Y. Zhang, J. Chao, J. Li, L. Wang, J. Lin, K. V. Gothelf and C. Fan, *Nat. Commun.*, 2019, **10**, 5597.

82 N. Li, Y. Shang, R. Xu, Q. Jiang, J. Liu, L. Wang, Z. Cheng and B. Ding, *J. Am. Chem. Soc.*, 2019, **141**, 17968–17972.
83 Y. Zhang, Z. Qu, C. Jiang, Y. Liu, R. Pradeep Narayanan, D. Williams, X. Zuo, L. Wang, H. Yan, H. Liu and C. Fan, *J. Am. Chem. Soc.*, 2021, **143**, 8639–8646.
84 Y. Chen, F. Fang and N. Zhang, *npj 2D Mater. Appl.*, 2024, **8**, 1–23.
85 Z. Cai, B. Liu, X. Zou and H.-M. Cheng, *Chem. Rev.*, 2018, **118**, 6091–6133.
86 X. Gao, L. Zheng, F. Luo, J. Qian, J. Wang, M. Yan, W. Wang, Q. Wu, J. Tang, Y. Cao, C. Tan, J. Tang, M. Zhu, Y. Wang, Y. Li, L. Sun, G. Gao, J. Yin, L. Lin, Z. Liu, S. Qin and H. Peng, *Nat. Commun.*, 2022, **13**, 5410.
87 S. M. Kim, A. Hsu, M. H. Park, S. H. Chae, S. J. Yun, J. S. Lee, D.-H. Cho, W. Fang, C. Lee, T. Palacios, M. Dresselhaus, K. K. Kim, Y. H. Lee and J. Kong, *Nat. Commun.*, 2015, **6**, 8662.
88 S. P. Surwade, F. Zhou, B. Wei, W. Sun, A. Powell, C. O'Donnell, P. Yin and H. Liu, *J. Am. Chem. Soc.*, 2013, **135**, 6778–6781.
89 J. E. Crowell, *J. Vac. Sci. Technol., A*, 2003, **21**, S88–S95.
90 G. N. Parsons and R. D. Clark, *Chem. Mater.*, 2020, **32**, 4920–4953.
91 R. W. Johnson, A. Hultqvist and S. F. Bent, *Mater. Today*, 2014, **17**, 236–246.
92 S. M. George, *Chem. Rev.*, 2010, **110**, 111–131.
93 G. Posnjak, X. Yin, P. Butler, O. Bienek, M. Dass, S. Lee, I. D. Sharp and T. Liedl, *Science*, 2024, **384**, 781–785.
94 L. Hui, C. Chen, M. A. Kim and H. Liu, *ACS Appl. Mater. Interfaces*, 2022, **14**, 16538–16545.
95 S. P. Surwade, S. Zhao and H. Liu, *J. Am. Chem. Soc.*, 2011, **133**, 11868–11871.
96 C. T. Diagne, C. Brun, D. Gasparutto, X. Baillin and R. Tiron, *ACS Nano*, 2016, **10**, 6458–6463.
97 J. Liu, Y. Geng, E. Pound, S. Gyawali, J. R. Ashton, J. Hickey, A. T. Woolley and J. N. Harb, *ACS Nano*, 2011, **5**, 2240–2247.
98 X. Dai, X. Chen, X. Jing, Y. Zhang, M. Pan, M. Li, Q. Li, P. Liu, C. Fan and X. Liu, *Angew. Chem., Int. Ed.*, 2022, **61**, e202114190.
99 J. Shen, W. Sun, D. Liu, T. Schaus and P. Yin, *Nat. Mater.*, 2021, **20**, 683–690.
100 R. L. Siegel, K. D. Miller, N. S. Wagle and A. Jemal, *Ca-Cancer J. Clin.*, 2023, **73**, 17–48.
101 C. E. Castro, F. Kilchherr, D.-N. Kim, E. L. Shiao, T. Wauer, P. Wortmann, M. Bathe and H. Dietz, *Nat. Methods*, 2011, **8**, 221–229.
102 D. Ye, X. Zuo and C. Fan, *Annu. Rev. Anal. Chem.*, 2018, **11**, 171–195.
103 J. Dai, C. Xing, Y. Lin, Y. Huang, Y. Yang, Z. Chen, C. Lu and H. Yang, *Sens. Actuators, B*, 2021, **344**, 130195.
104 Y. Ke, S. Lindsay, Y. Chang, Y. Liu and H. Yan, *Science*, 2008, **319**, 180–183.
105 E. Weinhold and B. Chakraborty, *Nanoscale*, 2021, **13**, 2465–2471.
106 M. Scherf, F. Scheffler, C. Maffeo, U. Kemper, J. Ye, A. Aksimentiev, R. Seidel and U. Reibetanz, *Nanoscale*, 2022, **14**, 18041–18050.
107 M. J. Urban, P. K. Dutta, P. Wang, X. Duan, X. Shen, B. Ding, Y. Ke and N. Liu, *J. Am. Chem. Soc.*, 2016, **138**, 5495–5498.
108 C. Wen, E. Bertosin, X. Shi, C. Dekker and S. Schmid, *Nano Lett.*, 2023, **23**, 788–794.
109 Y. Choi, C. Schmidt, P. Tinnefeld, I. Bald and S. Rödiger, *Sci. Rep.*, 2019, **9**, 4769.
110 J. J. Rossi, *Cell*, 2009, **137**, 990–992.
111 C. Xing, S. Chen, Q. Lin, Y. Lin, M. Wang, J. Wang and C. Lu, *Nanoscale*, 2022, **14**, 1327–1332.
112 V. Maingi, Z. Zhang, C. Thachuk, N. Sarraf, E. R. Chapman and P. W. K. Rothemund, *Nat. Commun.*, 2023, **14**, 1532.
113 W. Livernois, P. (Simon) Cao, S. Saha, Q. Ding, A. Gopinath and M. P. Anantram, *Nanotechnology*, 2024, **35**, 325202.
114 M. Tintoré, I. Gállego, B. Manning, R. Eritja and C. Fàbrega, *Angew. Chem., Int. Ed.*, 2013, **52**, 7747–7750.
115 J. A. Kretzmann, A. Liedl, A. Monferrer, V. Mykhailiuk, S. Beerkens and H. Dietz, *Nat. Commun.*, 2023, **14**, 1017.
116 J. Wang, Y. Li and G. Nie, *Nat. Rev. Mater.*, 2021, **6**, 766–783.
117 T. Wu, H. Wang, R. Tian, S. Guo, Y. Liao, J. Liu and B. Ding, *Angew. Chem., Int. Ed.*, 2023, **62**, e202311698.
118 W. Engelen, C. Sigl, K. Kadletz, E. M. Willner and H. Dietz, *J. Am. Chem. Soc.*, 2021, **143**, 21630–21636.
119 A. Comberlato, M. M. Koga, S. Nüssing, I. A. Parish and M. M. C. Bastings, *Nano Lett.*, 2022, **22**, 2506–2513.
120 J. Liu, B. Ding, X. Wu, C. Yang, H. Wang, X. Lu, Y. Shang, Q. Liu and J. Fan, *J. Am. Chem. Soc.*, 2023, **145**, 9343–9353.
121 T. Masubuchi, M. Endo, R. Iizuka, A. Iguchi, D. H. Yoon, T. Sekiguchi, H. Qi, R. Iinuma, Y. Miyazono, S. Shoji, T. Funatsu, H. Sugiyama, Y. Harada, T. Ueda and H. Tadakuma, *Nat. Nanotechnol.*, 2018, **13**, 933–940.
122 J. Hahn, L. Y. T. Chou, R. S. Sørensen, R. M. Guerra and W. M. Shih, *ACS Nano*, 2020, **14**, 1550–1559.
123 S. Julin, Nonappa, B. Shen, V. Linko and M. A. Kostiainen, *Angew. Chem., Int. Ed.*, 2021, **60**, 827–833.
124 S. Liu, Q. Jiang, X. Zhao, R. Zhao, Y. Wang, Y. Wang, J. Liu, Y. Shang, S. Zhao, T. Wu, Y. Zhang, G. Nie and B. Ding, *Nat. Mater.*, 2021, **20**, 421–430.
125 Q. Zhang, Q. Jiang, N. Li, L. Dai, Q. Liu, L. Song, J. Wang, Y. Li, J. Tian, B. Ding and Y. Du, *ACS Nano*, 2014, **8**, 6633–6643.
126 Q. Jiang, Y. Shang, Y. Xie and B. Ding, *Adv. Mater.*, 2024, **36**, e2301035.
127 H. Ijäs, I. Hakaste, B. Shen, M. A. Kostiainen and V. Linko, *ACS Nano*, 2019, **13**, 5959–5967.
128 S. M. Douglas, I. Bachelet and G. M. Church, *Science*, 2012, **335**, 831–834.
129 L. Li, J. Yin, W. Ma, L. Tang, J. Zou, L. Yang, T. Du, Y. Zhao, L. Wang, Z. Yang, C. Fan, J. Chao and X. Chen, *Nat. Mater.*, 2024, **23**, 993–1001.
130 L. Xin, C. Zhou, X. Duan and N. Liu, *Nat. Commun.*, 2019, **10**, 5394.

131 W. Fang, S. Jia, J. Chao, L. Wang, X. Duan, H. Liu, Q. Li, X. Zuo, L. Wang, L. Wang, N. Liu and C. Fan, *Sci. Adv.*, 2019, **5**, eaau4506.
132 K. Tapio, A. Mostafa, Y. Kanehira, A. Suma, A. Dutta and I. Bald, *ACS Nano*, 2021, **15**, 7065–7077.
133 Y. Kanehira, K. Tapio, G. Wegner, S. Kogikoski Jr., S. Rüstig, C. Prietzel, K. Busch and I. Bald, *ACS Nano*, 2023, **17**, 21227–21239.
134 S. Nam, N. Oh, Y. Zhai and M. Shim, *ACS Nano*, 2015, **9**, 878–885.
135 C. Chen, X. Wei, M. F. Parsons, J. Guo, J. L. Banal, Y. Zhao, M. N. Scott, G. S. Schlau-Cohen, R. Hernandez and M. Bathe, *Nat. Commun.*, 2022, **13**, 4935.
136 V. Glembockyte, L. Grabenhorst, K. Trofymchuk and P. Tinnefeld, *Acc. Chem. Res.*, 2021, **54**, 3338–3348.
137 L. Grabenhorst, K. Trofymchuk, F. Steiner, V. Glembockyte and P. Tinnefeld, *Methods Appl. Fluoresc.*, 2020, **8**, 024003.
138 R. Yaadav, K. Trofymchuk, F. Gong, X. Ji, F. Steiner, P. Tinnefeld and Z. He, *J. Phys. Chem. C*, 2024, **128**, 9154–9160.
139 O. S. Ojambati, R. Chikkaraddy, W. D. Deacon, M. Horton, D. Kos, V. A. Turek, U. F. Keyser and J. J. Baumberg, *Nat. Commun.*, 2019, **10**, 1049.
140 C. Zhou, X. Duan and N. Liu, *Acc. Chem. Res.*, 2017, **50**, 2906–2914.
141 K. Martens, F. Binkowski, L. Nguyen, L. Hu, A. O. Govorov, S. Burger and T. Liedl, *Nat. Commun.*, 2021, **12**, 2025.
142 A. Gopinath, E. Miyazono, A. Faraon and P. W. K. Rothemund, *Nature*, 2016, **535**, 401–405.
143 A. Gopinath, C. Thachuk, A. Mitskovets, H. A. Atwater, D. Kirkpatrick and P. W. K. Rothemund, *Science*, 2021, **371**, eabd6179.
144 S. Dey, C. Fan, K. V. Gothelf, J. Li, C. Lin, L. Liu, N. Liu, M. A. D. Nijenhuis, B. Saccà, F. C. Simmel, H. Yan and P. Zhan, *Nat. Rev. Methods Primers*, 2021, **1**, 1–24.
145 E. Benson, R. C. Marzo, J. Bath and A. J. Turberfield, *Sci. Rob.*, 2022, **7**, eabn5459.
146 X. R. Liu, I. Y. Loh, W. Siti, H. L. Too, T. Anderson and Z. Wang, *Nanoscale Horiz.*, 2023, **8**, 827–841.
147 J. List, M. Weber and F. C. Simmel, *Angew. Chem., Int. Ed.*, 2014, **53**, 4236–4239.
148 Y. Wang, I. Baars, I. Berzina, I. Rocamonde-Lago, B. Shen, Y. Yang, M. Lolaico, J. Waldvogel, I. Smyrlaki, K. Zhu, R. A. Harris and B. Högberg, *Nat. Nanotechnol.*, 2024, **19**, 1366–1374.
149 Y. Wang, J. V. Le, K. Crocker, M. A. Darcy, P. D. Halley, D. Zhao, N. Andrioff, C. Croy, M. G. Poirier, R. Bundschuh and C. E. Castro, *Nucleic Acids Res.*, 2021, **49**, 8987–8999.
150 A. Mills, N. Aissaoui, D. Maurel, J. Elezgaray, F. Morvan, J. J. Vasseur, E. Margeat, R. B. Quast, J. Lai Kee-Him, N. Saint, C. Benistant, A. Nord, F. Pedaci and G. Bellot, *Nat. Commun.*, 2022, **13**, 3182.
151 H. Gu, J. Chao, S.-J. Xiao and N. C. Seeman, *Nature*, 2010, **465**, 202–205.
152 A. J. Thubagere, W. Li, R. F. Johnson, Z. Chen, S. Doroudi, Y. L. Lee, G. Izatt, S. Wittman, N. Srinivas, D. Woods, E. Winfree and L. Qian, *Science*, 2017, **357**, eaan6558.
153 K. Lund, A. J. Manzo, N. Dabby, N. Michelotti, A. Johnson-Buck, J. Nangreave, S. Taylor, R. Pei, M. N. Stojanovic, N. G. Walter, E. Winfree and H. Yan, *Nature*, 2010, **465**, 206–210.
154 C. Zhou, X. Duan and N. Liu, *Nat. Commun.*, 2015, **6**, 8102.
155 W. Siti, H. L. Too, T. Anderson, X. R. Liu, I. Y. Loh and Z. Wang, *Sci. Adv.*, 2023, **9**, eadi8444.
156 P. Ketterer, E. M. Willner and H. Dietz, *Sci. Adv.*, 2016, **2**, e1501209.
157 F. Zhou, H. Ni, G. Zhu, L. Bershadsky, R. Sha, N. C. Seeman and P. M. Chaikin, *Sci. Rob.*, 2023, **8**, eadf1274.
158 E. Kopperger, J. List, S. Madhira, F. Rothfischer, D. C. Lamb and F. C. Simmel, *Science*, 2018, **359**, 296–301.
159 H. Lv, N. Xie, M. Li, M. Dong, C. Sun, Q. Zhang, L. Zhao, J. Li, X. Zuo, H. Chen, F. Wang and C. Fan, *Nature*, 2023, **622**, 292–300.
160 C. Truong-Quoc, J. Y. Lee, K. S. Kim and D.-N. Kim, *Nat. Mater.*, 2024, 1–9.
161 Z. Tang, Z.-X. Yin, J.-Z. Cui, J. Yang and R.-S. Wang, *J. Nanoelectron. Optoelectron.*, 2021, **16**, 534–545.
162 Y. Liu, X. Hu, T. Fu, R. Wang and W. Tan, *Sci. China: Chem.*, 2019, **62**, 407–408.
163 C. Truong-Quoc, J. Y. Lee, K. S. Kim and D.-N. Kim, *Nat. Mater.*, 2024, **23**, 984–992.
164 M. C. Liu, G. R. Oxnard, E. A. Klein, C. Swanton, M. V. Seiden and CCGA Consortium, *Ann. Oncol.*, 2020, **31**, 745–759.
165 L. Yang, Q. Tang, M. Zhang, Y. Tian, X. Chen, R. Xu, Q. Ma, P. Guo, C. Zhang and D. Han, *Nat. Commun.*, 2024, **15**, 4583.
166 Y. Amir, E. Ben-Ishay, D. Levner, S. Ittah, A. Abu-Horowitz and I. Bachelet, *Nat. Nanotechnol.*, 2014, **9**, 353–357.
167 Y. Zhang, F. Wang, J. Chao, M. Xie, H. Liu, M. Pan, E. Kopperger, X. Liu, Q. Li, J. Shi, L. Wang, J. Hu, L. Wang, F. C. Simmel and C. Fan, *Nat. Commun.*, 2019, **10**, 5469.
168 S. Fan, D. Wang, J. Cheng, Y. Liu, T. Luo, D. Cui, Y. Ke and J. Song, *Angew. Chem., Int. Ed.*, 2020, **59**, 12991–12997.
169 C. Jiang, R. Tan, W. Li, Y. Zhang and H. Liu, *Small*, 2024, **20**, 2406470.
170 W. Jiang, J. Li, Z. Lin, J. Guo, J. Ma, Z. Wang, M. Zhang and Y. Wu, *Small Struct.*, 2023, **4**, 2200376.
171 F. Praetorius, B. Kick, K. L. Behler, M. N. Honemann, D. Weuster-Botz and H. Dietz, *Nature*, 2017, **552**, 84–87.
172 Y. Jia, L. Chen, J. Liu, W. Li and H. Gu, *Chem*, 2021, **7**, 959–981.
173 A. Bednarz, S. M. Sønderskov, M. Dong and V. Birkedal, *Nanoscale*, 2023, **15**, 1317–1326.
174 S. Ramakrishnan, G. Krainer, G. Grundmeier, M. Schlierf and A. Keller, *Small*, 2017, **13**, 1702100.

175 V. Linko and A. Keller, *Small*, 2023, **19**, 2301935.
176 F. Matter, A. L. Luna and M. Niederberger, *Nano Today*, 2020, **30**, 100827.
177 Y. Xin, S. Martinez Rivadeneira, G. Grundmeier, M. Castro and A. Keller, *Nano Res.*, 2020, **13**, 3142–3150.
178 M. Hanke, N. Hansen, R. Chen, G. Grundmeier, K. Fahmy and A. Keller, *Int. J. Mol. Sci.*, 2022, **23**, 2817.
179 V. Linko, J. Mikkilä and M. A. Kostiainen, in *Virus-Derived Nanoparticles for Advanced Technologies: Methods and Protocols*, ed. C. Wege and G. P. Lomonossoff, Springer, New York, NY, 2018, pp. 267–277.
180 F. M. Anastassacos, Z. Zhao, Y. Zeng and W. M. Shih, *J. Am. Chem. Soc.*, 2020, **142**, 3311–3315.
181 N. A. Estrich, A. Hernandez-Garcia, R. de Vries and T. H. LaBean, *ACS Nano*, 2017, **11**, 831–842.
182 J. A. Kretzmann, A. Liedl, A. Monferrer, V. Mykhailiuk, S. Beerkens and H. Dietz, *Nat. Commun.*, 2023, **14**, 1017.
183 O. Kovecses, F. E. Mercier and M. McKeague, *Leukemia*, 2024, **38**, 1441–1454.
184 B. R. Janakaloti Narayanareddy, N. R. Allipeta, J. Allard and S. P. Gross, *Commun. Biol.*, 2024, **7**, 1–10.
185 B. Wang, S. Hu, Y. Teng, J. Chen, H. Wang, Y. Xu, K. Wang, J. Xu, Y. Cheng and X. Gao, *Signal Transduction Targeted Ther.*, 2024, **9**, 1–65.
186 Y. C. Zeng, O. J. Young, C. M. Wintersinger, F. M. Anastassacos, J. I. MacDonald, G. Isinelli, M. O. Dellacherie, M. Sobral, H. Bai, A. R. Graveline, A. Vernet, M. Sanchez, K. Mulligan, Y. Choi, T. C. Ferrante, D. B. Keskin, G. G. Fell, D. Neuberg, C. J. Wu, D. J. Mooney, I. C. Kwon, J. H. Ryu and W. M. Shih, *Nat. Nanotechnol.*, 2024, **19**, 1055–1065.